Journal of Organometallic Chemistry, 369 (1989) 393–417
Elsevier Sequoia S.A., Lausanne – Printed in The Netherlands
JOM 09700

Cluster chemistry

LX *. Reactions of the complex $Ru_5(\mu_5\text{-}\eta^2,P\text{-}C_2PPh_2)(\mu\text{-}PPh_2)(CO)_{13}$ with CO or dihydrogen. X-Ray crystal structures of $Ru_5(\mu\text{-}H)(\mu_5\text{-}CCHPPh_2)(\mu\text{-}PPh_2)(CO)_{13}$, $Ru_5(\mu\text{-}H)_2(\mu_4\text{-}CCH_2PPh_2)(\mu\text{-}PPh_2)(CO)_{12}$ and $Ru_5C(\mu\text{-}H)_3(\mu\text{-}PPh_2)(CO)_{11}(PMePh_2)$

Michael I. Bruce, Michael L. Williams,

Jordan Laboratories, Department of Physical and Inorganic Chemistry, University of Adelaide, Adelaide, South Australia 5001 (Australia)

Brian W. Skelton and Allan H. White

Department of Physical and Inorganic Chemistry, University of Western Australia, Nedlands, Western Australia 6009 (Australia)

(Received November 25th, 1988)

Abstract

The complex $Ru_5(\mu_5\text{-}C_2PPh_2)(\mu\text{-}PPh_2)(CO)_{13}$ (**2**) reacts with CO (10 atm, 25 °C, 36 h) to give $Ru_5(\mu_5\text{-}C_2PPh_2)(\mu\text{-}PPh_2)(CO)_{15}$, which is converted under CO (12 atm, 70 °C, 22 h) into an isomeric cluster, both clusters containing Ru_2-spiked Ru_3 cores. Under more vigorous conditions (20 atm, 100 °C, 16 h), $Ru_4(\mu_4\text{-}C_2)(\mu\text{-}PPh_2)_2(CO)_{12}$, containing a C_2 molecule bridging two $Ru_2(\mu\text{-}PPh_2)(CO)_6$ moieties, is formed. Complex **2** reacts with H_2 (1 atm, 80 °C, 5 h) to give successively $Ru_5(\mu\text{-}H)(\mu_5\text{-}CCHPPh_2)(\mu\text{-}PPh_2)(CO)_{13}$ (**13**), $Ru_5(\mu\text{-}H)_2(\mu_4\text{-}CCH_2PPh_2)(\mu\text{-}PPh_2)(CO)_{12}$ (**14**), and $Ru_5C(\mu\text{-}H)_3(\mu\text{-}PPh_2)(CO)_{11}(PMePh_2)$ (**15**), the C≡C triple bond thereby being reduced to $(C + CH_3)$. Under pressure (10 atm, 25 °C, 18 h), a mixture of $Ru_4(\mu\text{-}H)_3(\mu_4\text{-}HC_2PPh_2)(\mu\text{-}PPh_2)(CO)_{10}$ and $Ru_4(\mu\text{-}H)_4(CO)_{12}$ is formed. The molecular structures and transformations of these complexes are discussed. Crystal data for **13**: monoclinic, space group $P2_1/n$, a 25.115(6), b 10.126(2), c 17.373(4) Å, β 109.88(2)°, $Z = 4$; 9411 observed data were refined to $R = 0.038$, $R' = 0.032$; **14**: triclinic, space group $P\bar{1}$, a 16.98(1), b 12.171(4), c 10.762(5) Å, α 71.16(4), β 87.20(4), γ 72.23(5)°, $Z = 2$; 6312 observed data were

* For Part LIX, see ref. 44.

0022-328X/89/$03.50

refined to $R = 0.063$, $R' = 0.085$; **15**: triclinic, space group $P\bar{1}$, a 18.658(4), b 12.483(3), c 9.678(2) Å, α 69.13(2), β 78.21(2), γ 73.19(2)°, $Z = 2$; 10214 observed data were refined to $R = 0.026$, $R' = 0.029$.

Introduction

We recently described the radical-initiated reaction between $Ru_3(CO)_{12}$ and $C_2(PPh_2)_2$(dppa) to give $\{Ru_3(CO)_{11}\}_2(\mu$-dppa) (**1**), and the thermal condensation of **1** to give the pentanuclear cluster $Ru_5(\mu_5\text{-}\eta^2, P\text{-}C_2PPh_2)(\mu\text{-}PPh_2)(CO)_{13}$ (**2**) in 88% yield [1]. The latter complex was described independently by Daran and coworkers [2], who isolated it from the thermal reaction between $Ru_3(CO)_{12}$ and dppa in tetrahydrofuran; two other complexes obtained from this reaction were characterised as the tetranuclear complexes $Ru_4(\mu_4\text{-}PPh)(\mu_4\text{-}\eta^2, P\text{-}PhC_2PPh_2)(CO)_{10}$ (**3**), and $\{Ru_2(\mu\text{-}PPh_2)(\mu\text{-}C_2PPh_2)(CO)_5\}_2$ (**4**) [3]. More recently, the osmium analogues of **1** and **2** were reported [4]. Earlier related work by Carty and coworkers with PhC_2PPh_2 resulted in the formation of $Ru_3(CO)_{11}\{PPh_2(C_2Ph)\}$ (**5**) by the ETC reaction of the ligand with $Ru_3(CO)_{12}$, and its thermal conversion into $Ru_5(\mu_4\text{-}C_2Ph)(\mu\text{-}PPh_2)(CO)_{13}$ (**6**), which was formed in 30% yield, together with the binuclear complex $Ru_2(\mu\text{-}PPh_2)(\mu\text{-}C_2Ph)(CO)_6$ [5]. Further reaction of **6** with CO (1 atm, room temperature) rapidly gave $Ru_5(\mu_5\text{-}C_2Ph)(\mu\text{-}PPh_2)(\mu\text{-}CO)(CO)_{13}$ (**7**; Scheme 1), containing an open Ru_5 framework similar to that found in **2**. Complex **7** readily loses CO to regenerate **6**, and evidence for reversible addition of other ligands such as nitriles, amines, or pyridine to **6** was also obtained. The square pyramidal Ru_5 framework in **6** is also opened by addition of PhC_2C_2Ph, to give $Ru_5(\mu_5\text{-}C_2Ph)(\mu_3\text{-}PhCCC_2Ph)(\mu\text{-}PPh_2)(CO)_{12}$ (**8**; Scheme 1) [6].

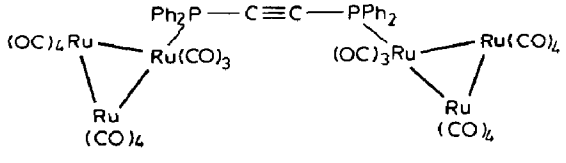

(1)

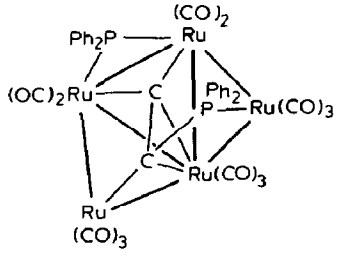

(2)

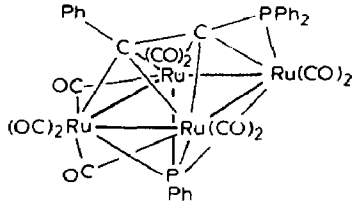

(3)

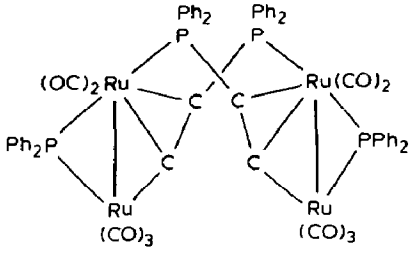

(4)

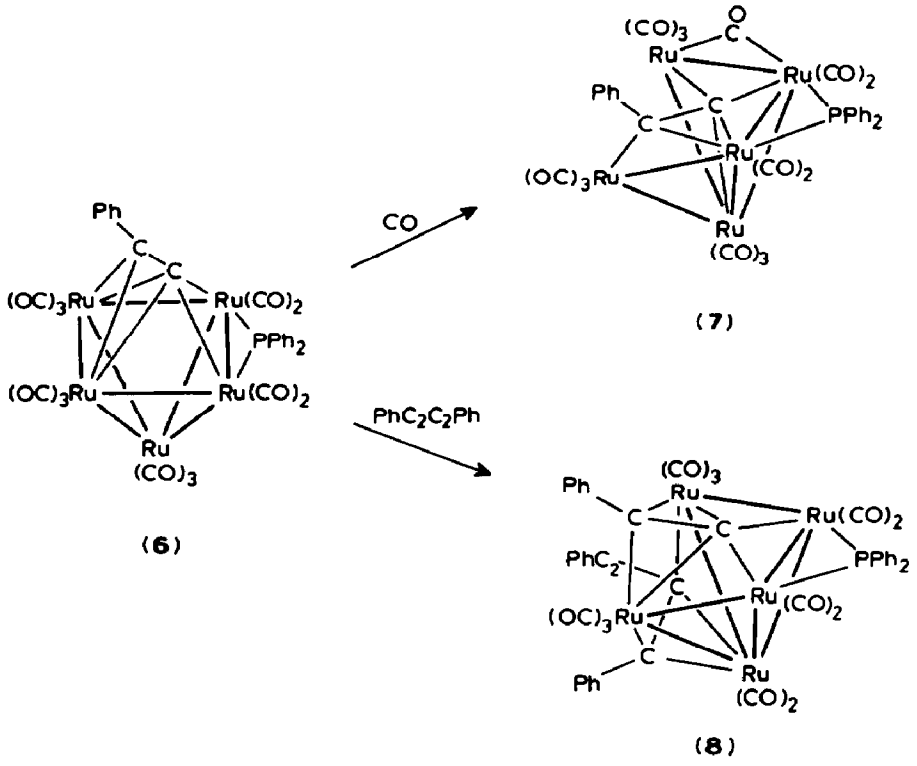

Scheme 1

The characteristic facile P–C(*sp*) bond cleavage reactions observed with these complexes [7] allows the formation of cluster-bonded acetylide ligands which interact with several metal atoms: in **2**, for example, the phosphinoacetylide is attached to all five metal atoms of the open Ru_5 cluster, the acetylide group being bonded to four of them and the PPh_2 group to the fifth; in **7** and **8**, the PhC_2 ligand interacts with all five metal atoms.

The reactivity of cluster-bound molecules depends on the number of metal atoms with which the fragment interacts and on the degree of encapsulation of the fragment. Thus, fully enclosed interstitial atoms, such as the carbon atoms in $Ru_6C(CO)_{17}$, seem to be protected, while unusually high reactivity may be observed for partially exposed atoms, such as that found in $[Fe_4C(CO)_{12}]^{2-}$ [8]. Similarly, a μ_4-acetylide ligand appears to be more reactive than the corresponding μ_3-acetylide, although precise comparisons are not always possible.

Our discovery of a high-yield route to **2** enabled us to examine some of its reactions in detail. We have briefly described the formation of two isomers of $Ru_5(\mu_5\text{-}C_2PPh_2)(\mu\text{-}PPh_2)(CO)_{15}$ (**9** and **10**) in the reaction with CO (Scheme 2) [9], and the formation of $Ru_4(\mu_4\text{-}C_2)(\mu\text{-}PPh_2)_2(CO)_{12}$ (**11**), which contains a C_2 ligand [10], and have shown that with dihydrogen partial breakdown of the Ru_5 cluster gives $Ru_4(\mu\text{-}H)_3(\mu_4\text{-}HC_2PPh_2)(\mu\text{-}PPh_2)(CO)_{10}$ (**12**) [11]; under mild conditions, stepwise hydrogenation of the phosphinoacetylide ligand (Scheme 2) gives successively $Ru_5(\mu\text{-}H)(\mu_5\text{-}CCHPPh_2)(\mu\text{-}PPh_2)(CO)_{13}$ (**13**), $Ru_5(\mu\text{-}H)_2(\mu_5\text{-}CCH_2PPh_2)(\mu\text{-}PPh_2)(CO)_{12}$ (**14**) and $Ru_5C(\mu\text{-}H)_3(\mu\text{-}PPh_2)(CO)_{11}(PMePh_2)$ (**15**) [12]. This paper expands on those preliminary accounts, giving full details of the

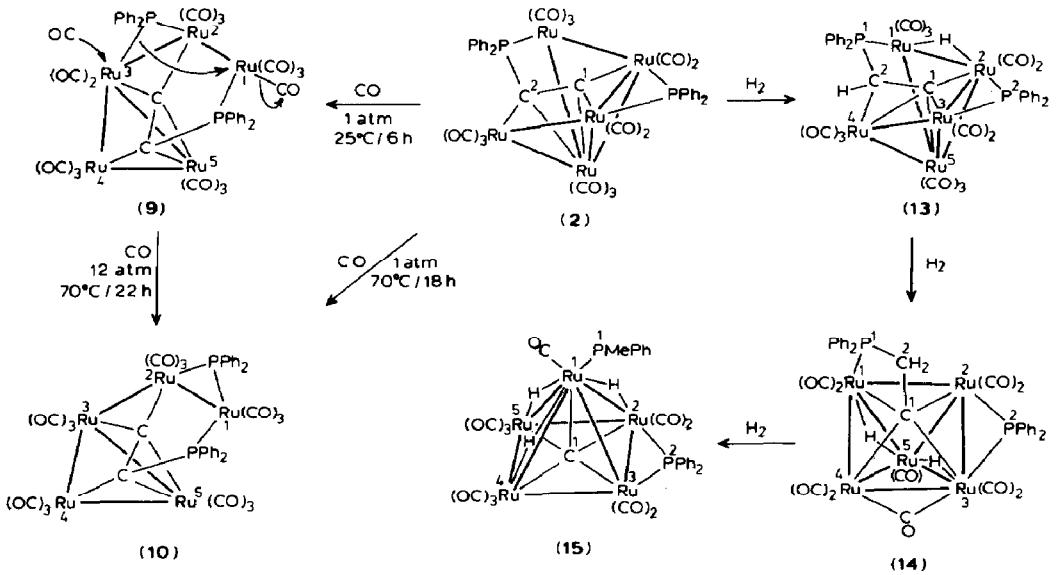

Scheme 2

syntheses, and discussing in greater depth the crystallographic studies. The X-ray structure of **14** is reported for the first time.

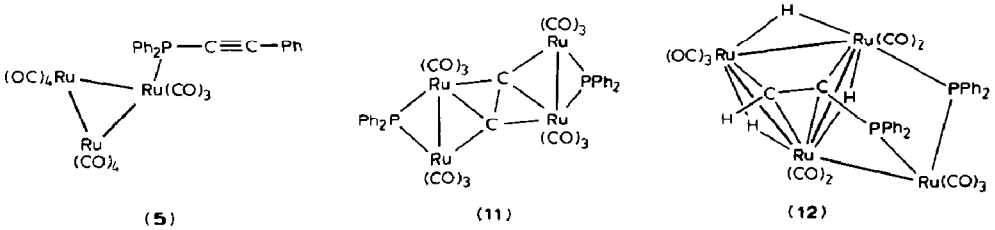

Results

Reactions between 2 and CO

Two isomeric complexes of composition $Ru_5(\mu_5\text{-}\eta^2,P\text{-}C_2PPh_2)(\mu\text{-}PPh_2)(CO)_{15}$ were obtained from the reaction between **2** and CO in cyclohexane. Under mild conditions (25 °C, 1 atm, 6 h), a dark red complex **9** separates out in high yield, while after 18 h reaction at 70 °C, a second red complex **10** can be isolated in 35% yield. Interconversion of the two complexes cannot be achieved directly by heating, but under CO (70 °C, 12 atm), **9** is transformed into **10** in 22 h. The molecular structures of **9** and **10** have been determined by X-ray crystallography.

The two complexes contain the same Ru_5 skeleton in the form of an Ru_3 triangle spiked by an Ru_2 chain. This can be formed by the breaking of two of the Ru–Ru bonds in the Ru_5 core of **2**, and is consistent with the addition of two 2e donor ligands. In both, the phosphinoacetylide ligand is attached to Ru(1) by a normal 2e donor interaction with P(1), and to the Ru(3)Ru(4)Ru(5) triangle by the familiar $\mu_3\text{-}\eta^2$ (||) attachment of the acetylide unit. There is a weak interaction between

Ru(2) and C(2) (2.324(4) Å in **9**, 2.261(7) Å in **10**). The Ru(4)–Ru(5) distances in **9** and **10**, bridged by C(1) of the acetylide group, are remarkably short (2.670(1), 2.675(1) Å). The separation compares with that of 2.665(3) Å found in $[Ru_3(\mu_3\text{-}C_2Bu^t)(CO)_9]^-$ [13].

The major differences are the bridging of Ru(2)–Ru(3) by P(2) in **9**, while in **10**, P(2) bridges Ru(1)–Ru(2); Ru(1) has four CO groups in **9** and three in **10**, while Ru(3) has two CO groups in **9** but three in **10**. As pointed out earlier, the Ru(1)–Ru(2) interaction in **9** is of the unsupported donor–acceptor type (3.009(1) Å), Ru(1) acquiring the normal 18e configuration from P(1) and four CO ligands. Several osmium complexes containing Os → Os bonds of this type have been prepared by Pomeroy and coworkers [14]; in both cases above, the metal atom separation is considerably larger than those in $M_3(CO)_{12}$ (M = Ru or Os).

The major structural changes resulting from the conversion of **9** into **10** are found in a marked shortening of Ru(1)–Ru(2) (by 0.12 Å) and of Ru(3)–Ru(4) (by 0.08 Å), and of the Ru(2)–C(2) interaction (from 2.324(4) Å in **9** to 2.261(7) Å in **10**). At the same time, the Ru(4)–C(2) separation increases (from 2.281(4) Å in **9** to 2.359(7) Å in **10**); that is, the alkyne ligands has shifted so that C(1)–C(2) has become nearly parallel with Ru(3)–Ru(4). In addition, the Ru(2)Ru(3)P(2) bridge in **9** shows a considerable asymmetry (Ru–P 2.261(1), 2.360(1), av. 2.310 Å), contrasting with the symmetrical arrangement in **10** (Ru–P 2.314(2), 2.316(2) Å). This difference probably results from the strong *trans* effect of the RuL_5 group.

Scheme 1 depicts the conversion of **2** into **9**, and suggests a route by which **9** is transformed into **10** that takes account of the observation that the 'isomerisation' does not proceed unless free CO is present. Addition of CO at Ru(3) results in displacement of P(2), which in turn displaces one CO ligand from Ru(1), while pivoting on Ru(2) throughout the isomerisation. The formation of **9** from **2** by addition of two CO groups results from the cleavage of two Ru–Ru bonds and the formation of a novel alkyne, Ru(2)–C≡C–P(1); conversion of **9** into **10** results in a more regular distribution of electron density within the cluster and associated bridging ligands. The reaction is thus a classic example of the formation of a 'kinetic' isomer (**9**) and its subsequent transformation to the 'thermodynamic' form (**10**), but with the interesting variation of catalysis by CO.

A further effect of the isomerisation is to increase the thermal stability of **10**; solutions of **9** readily lose CO to regenerate **2**, while solutions of **10** require heating (42 °C, 7 h) before CO is lost to give **2**.

The ready mobility of ligands such as CO on cluster complexes makes the detailed course of these novel reactions uncertain. The frequently expressed suggestion [14] that bridging PR_2 groups may hold clusters intact during their reactions is again called into question [15,16] by the results depicted above: while the metal skeleton is essentially unaltered, the PPh_2 group migrates to a second site, remaining bonded to Ru(2) during this process. Such reactions, in which opening of the Ru_2P group generates a further coordination site, have implications for the role of such groups in cluster-catalysed reactions.

Under more severe reaction conditions (20 atm CO, 100 °C, 16 h), complex **2** is converted into the novel tetranuclear complex, $Ru_4(\mu_4\text{-}C_2)(\mu\text{-}PPh_2)_2(CO)_{12}$ (**11**). This derivative contains the C_2 ligand acting as a $2\eta^1,2\eta^2$-bridging unit between two $\{Ru_2(\mu\text{-}PPh_2)(CO)_6\}$ moieties, and as such, shows some resemblence to $Ru_2(\mu\text{-}PPh_2)(\mu\text{-}C_2Bu^t)(CO)_6$ (**16**) [17] or $\{Ru_2(\mu\text{-}PPh_2)(\mu\text{-}C_2Ph)(CO)_5\}_2$ (**4**) [3]. However,

Table 1. Non-hydrogen atomic coordinates *

	$Ru_5(\mu\text{-}H)(\mu_5\text{-}CCHPPh_2)(\mu\text{-}PPh_2)(CO)_{13}$ (13)			$Ru_5(\mu\text{-}H_2)(\mu_4\text{-}CCH_2PPh_2)(\mu\text{-}PPh_2)(CO)_{12}$ (14)			$Ru_5C(\mu\text{-}H)_3(\mu\text{-}PPh_2)(CO)_{11}(PMePh_2)$ (15)		
Atom	x	y	z	x	y	z	x	y	z
Ru(1)	0.08062(1)	0.22308(3)	0.21518(2)	0.25721(7)	0.35756(9)	0.17942(9)	0.23620(1)	0.35698(2)	0.14980(2)
Ru(2)	0.15044(1)	0.19045(3)	0.39754(2)	0.31209(7)	0.18353(10)	0.42313(10)	0.26849(1)	0.15544(2)	0.40322(2)
Ru(3)	0.13941(1)	-0.05961(3)	0.45652(2)	0.16066(6)	0.22895(9)	0.51792(9)	0.32464(1)	0.13204(2)	0.12489(2)
Ru(4)	0.04957(1)	-0.15768(3)	0.32264(2)	0.09363(6)	0.39513(9)	0.27533(10)	0.39013(1)	0.33407(2)	0.03169(2)
Ru(5)	0.13958(1)	-0.02193(3)	0.29284(2)	0.18292(7)	0.15964(10)	0.27925(10)	0.34515(1)	0.34482(2)	0.33249(2)
P(1)	-0.00130(4)	0.15586(11)	0.24533(6)	0.2629(2)	0.5285(3)	0.2249(3)	0.14918(4)	0.53839(6)	0.12753(8)
C(111)	-0.0327(2)	0.2938(4)	0.2828(2)	0.3612(8)	0.5593(11)	0.2319(12)	0.1046(1)	0.5744(2)	0.2974(3)
C(112)	-0.0234(2)	0.3169(5)	0.3645(3)	0.3858(10)	0.5860(15)	0.3370(15)	0.1092(2)	0.4897(3)	0.4375(3)
C(113)	-0.0495(2)	0.4177(5)	0.3895(3)	0.4553(12)	0.6190(17)	0.3342(18)	0.0761(2)	0.5169(3)	0.5655(4)
C(114)	-0.0843(2)	0.5012(6)	0.3355(3)	0.5004(10)	0.6295(16)	0.2289(20)	0.0371(2)	0.6316(3)	0.5545(4)
C(115)	-0.0925(2)	0.4850(6)	0.2542(3)	0.4778(11)	0.6048(17)	0.1218(18)	0.0310(2)	0.7170(3)	0.4186(5)
C(116)	-0.0676(2)	0.3818(5)	0.2273(3)	0.4083(10)	0.5707(15)	0.1253(15)	0.0648(2)	0.6889(3)	0.2906(4)
C(121)	-0.0646(2)	0.0853(4)	0.1708(2)	0.1961(8)	0.6783(11)	0.1407(12)	0.1915(2)	0.6630(2)	0.0280(3)
C(122)	-0.0782(2)	0.1003(5)	0.0883(3)	0.1685(9)	0.7109(13)	0.0106(13)	0.2333(2)	0.6960(3)	0.1039(4)
C(123)	-0.1293(2)	0.0521(5)	0.0335(3)	0.1219(11)	0.8287(14)	-0.0539(14)	0.2707(2)	0.7849(3)	0.0304(5)
C(124)	-0.1658(2)	-0.0081(5)	0.0628(3)	0.1030(10)	0.9161(13)	0.0035(6)	0.2667(2)	0.8424(3)	-0.1185(5)
C(125)	-0.1530(2)	-0.0264(6)	0.1454(3)	0.1288(10)	0.8852(13)	0.1333(16)	0.2261(3)	0.8125(4)	-0.1941(4)
C(126)	-0.1029(2)	0.0209(6)	0.1986(3)	0.1762(9)	0.7690(12)	0.1992(13)	0.1880(2)	0.7220(3)	-0.1226(4)
C(1)	0.0249(2)	0.0463(4)	0.3306(2)	0.2315(7)	0.4575(15)	0.3948(12)	0.0679(2)	0.5681(3)	0.0303(5)
C(2)	0.0856(2)	0.0382(4)	0.3605(2)	0.2147(8)	0.3593(11)	0.3758(12)	0.3354(1)	0.2394(2)	0.2233(3)
P(2)	0.21422(6)	0.08095(11)	0.50846(7)	0.2745(2)	0.0671(3)	0.6123(3)	0.24282(4)	0.03182(5)	0.29985(7)
C(211)	0.2837(2)	0.0318(4)	0.5067(2)	0.3158(9)	0.0487(12)	0.7757(11)	0.1485(2)	0.0557(2)	0.2518(3)
C(212)	0.3176(2)	0.1117(5)	0.4804(3)	0.3116(11)	-0.0498(15)	0.8825(12)	0.1401(2)	0.0353(3)	0.1246(4)
C(213)	0.3701(2)	0.0717(6)	0.4796(3)	0.3424(12)	-0.0630(16)	1.0040(13)	0.0692(2)	0.0482(4)	0.0899(5)
C(214)	0.3892(2)	-0.0492(5)	0.5057(3)	0.3767(11)	0.0158(16)	1.0214(12)	0.0068(2)	0.0826(4)	0.1789(5)
C(215)	0.3566(2)	-0.1323(5)	0.5322(4)	0.3803(13)	0.1145(16)	0.9157(16)	0.0134(2)	0.1034(4)	0.3039(5)
C(216)	0.3043(2)	-0.0915(5)	0.5326(3)	0.3495(12)	0.1306(16)	0.7938(13)	0.0849(2)	0.0902(4)	0.3402(4)
C(221)	0.2312(2)	0.1573(5)	0.6092(3)	0.2837(9)	-0.0914(12)	0.6311(11)	0.2684(2)	-0.1276(2)	0.3907(3)

C(222)	0.1882(3)	0.1823(6)	0.6400(3)	0.2159(10)	-0.1310(14)	0.6189(14)	0.3399(2)	-0.1814(3)	0.4355(3)
C(223)	0.2013(3)	0.2443(7)	0.7177(4)	0.2297(13)	-0.2540(15)	0.6332(16)	0.3589(2)	-0.3007(3)	0.5147(4)
C(224)	0.2543(3)	0.2729(9)	0.7628(4)	0.3086(14)	-0.3331(15)	0.6560(19)	0.3074(2)	-0.3682(3)	0.5494(4)
C(225)	0.2922(3)	0.2457(10)	0.7344(4)	0.3762(13)	-0.2957(15)	0.6663(18)	0.2366(2)	-0.3172(3)	0.5044(4)
C(226)	0.2825(3)	0.1851(8)	0.6582(4)	0.3625(10)	-0.1757(10)	0.6533(15)	0.2168(2)	-0.1977(3)	0.4250(3)
C(11)	0.0605(2)	0.1389(5)	0.1109(3)	0.2546(10)	0.4059(11)	-0.0066(14)	0.1858(2)	0.3244(2)	0.0274(3)
O(11)	0.0477(2)	0.0970(5)	0.9461(2)	0.2558(9)	0.4365(11)	-0.1194(11)	0.1494(1)	0.3148(2)	-0.0483(3)
C(12)	0.1487(2)	0.2908(5)	0.2021(3)	0.3718(10)	0.2931(13)	0.1838(12)	-	-	-
O(12)	0.1863(1)	0.3405(4)	0.1913(2)	0.4425(6)	0.2617(11)	0.1708(11)	-	-	-
C(13)	0.0467(2)	0.3896(4)	0.1782(3)	-	-	-	-	-	-
O(13)	0.0296(2)	0.4884(4)	0.1525(3)	-	-	-	-	-	-
C(21)	0.1272(2)	0.3110(4)	0.4611(3)	0.3904(9)	0.2391(13)	0.4842(13)	0.3385(2)	0.0448(3)	0.5277(3)
O(21)	0.115(2)	0.3845(3)	0.4980(2)	0.4357(7)	0.2785(10)	0.5159(11)	0.3830(1)	-0.0180(2)	0.6030(3)
C(22)	0.2043(2)	0.3148(5)	0.3852(9)	0.4016(9)	0.0568(13)	0.3922(14)	0.1944(2)	0.1585(3)	0.5700(3)
O(22)	0.2363(1)	0.3904(4)	0.3811(2)	0.4542(7)	-0.0157(10)	0.3722(11)	0.1501(1)	0.1604(3)	0.6682(3)
C(31)	0.1021(2)	-0.0493(5)	0.5313(3)	0.1577(8)	0.3128(12)	0.6402(13)	0.4099(2)	0.0063(3)	0.1410(3)
O(31)	0.0783(2)	-0.0437(5)	0.5765(2)	0.1601(7)	0.3644(10)	0.7088(10)	0.4634(1)	-0.0665(2)	0.1520(3)
C(32)	0.1699(2)	-0.2252(5)	0.5009(3)	0.0859(9)	0.1480(12)	0.6175(13)	0.3081(2)	0.1206(2)	-0.0585(3)
O(32)	0.1873(2)	-0.3273(3)	0.5266(2)	0.0417(7)	0.1030(10)	0.6790(10)	0.2986(2)	0.1152(2)	-0.1673(3)
C(41)	-0.0015(2)	-0.2025(5)	0.2156(3)	0.0492(8)	0.5649(13)	0.2480(12)	0.4145(2)	0.4861(3)	-0.0504(3)
O(41)	-0.0295(2)	-0.2314(4)	0.1521(2)	0.0147(6)	0.6670(9)	0.2291(11)	0.4275(2)	0.5760(2)	-0.1045(3)
C(42)	0.0030(2)	-0.2084(5)	0.3836(3)	0.0104(10)	0.3974(15)	0.1620(16)	0.4900(2)	0.2429(3)	0.0690(3)
O(42)	-0.0236(2)	-0.2332(4)	0.4225(3)	-0.0404(8)	0.3974(13)	0.0961(12)	0.5481(1)	0.1858(2)	0.0927(3)
C(43)	0.0873(2)	-0.3264(5)	0.3364(3)	0.0198(9)	0.3657(14)	0.4178(12)	0.4014(2)	0.3107(3)	-0.1566(3)
O(43)	0.1064(2)	-0.4287(3)	0.3442(2)	-0.0416(7)	0.3717(12)	0.4701(12)	0.4114(2)	0.3017(2)	-0.2715(3)
C(51)	0.1086(2)	-0.1124(5)	0.1925(3)	0.2560(10)	-0.0026(14)	0.3103(12)	0.3831(2)	0.4864(3)	0.2732(3)
O(51)	0.0932(2)	-0.1698(4)	0.1314(2)	0.2965(8)	-0.1019(9)	0.3238(10)	0.4077(2)	0.5653(2)	0.2410(3)
C(52)	0.2047(1)	0.0577(5)	0.2791(3)	0.0903(10)	0.1131(15)	0.3547(15)	0.2889(2)	0.3559(2)	0.5183(3)
O(52)	0.2452(2)	0.0960(4)	0.2712(3)	0.0315(8)	0.0873(12)	0.3870(12)	0.2555(1)	0.3684(2)	0.6260(2)
C(53)	0.1868(2)	-0.1659(5)	0.3428(3)	0.1445(11)	0.1827(14)	0.1057(14)	0.4342(2)	0.2448(3)	0.4224(4)
O(53)	0.2178(2)	-0.2529(4)	0.3640(2)	0.1247(10)	0.1962(12)	0.0012(10)	0.4856(2)	0.1865(3)	0.4779(4)

* In (13): H(12); 0.100(1), 0.276(3), 0.317(2); H(1), 0.008(1), 0.056(4), 0.367(2)
(Core atoms for (14) not located) H(1a, b) estimated at (0.275, 0.430, 0.461; 0.184, 0.508, 0.420)
In (15): H(12): 0.190(2), 0.278(3), 0.311(4); H(14), 0.390(2), 0.428(3), -0.003(4); H(15), 0.262(2), 0.435(3), 0.246(4)

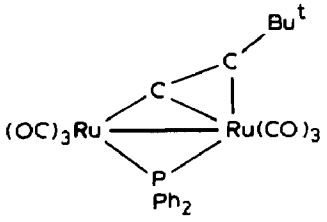

(16)

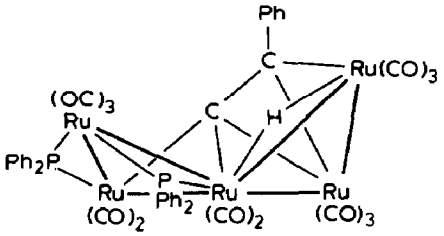

(17)

closer inspection of the C_2 ligand and its mode of interaction with the four metal atoms shows that this system has several unusual features. The dihedral angle between the two planes formed by the C_2 unit and the ruthenium with which it interacts in the η^2 mode is ca. 168°, a situation far removed from the nearly orthogonal arrangement found in $Co_2(\mu\text{-}\eta^2\text{-}C_2R_2)(CO)_6$ complexes, for example [18]. The implied weak Ru–C_2 π-bonding is reflected in long Ru–C distances (2.326(6), 2.470(6) Å), a short C–C bond (1.275(11) Å), and a small bend-back angle at the acetylenic carbons (157.4°). Similarly, the Ru–C σ-bond is long (at 2.065(5) Å), particularly when compared with those found in $Ru_3(\mu\text{-H})(\mu_3\text{-}C_2Bu^t)(CO)_9$ (1.947(3) Å) [19] or $Ru(C_2Ph)(PPh_3)_2(\eta\text{-}C_5H_5)$ (2.016(3) Å) [20].

The complexes containing C_2 ligands reported to date have various structures, ranging from the dicarbyne found in $(Bu^tO)_3W{\equiv}C{-}C{\equiv}W(OBu^t)_3$ [21], through the dicarbene in $(silox)_3Ta{=}C{=}C{=}Ta(silox)_3$ (silox = $OSiBu^t_3$) [22], to the acetylide dianions found in $L_nM{-}C{\equiv}C{-}ML_n$ (ML_n = $Re(CO)_5$ [23], $MCl(PMe_3)_2$ (M = Pd, Pt) [24], $Au(PR_3)$ [25]). The only other example of a C_2 unit bridging more than two metals is found in *trans*-$Pt\{C_2W_2(OBu^t)_5\}_2(PMe_2Ph)_2$ and related complexes, which are considered to contain an ethene tetraanion: the C–C separation is 1.336(13) Å, with Pt–C–C angles of 143.9(8)° [26]. Where observed, the ^{13}C NMR resonances of the C_2 ligands mentioned above are consistent with the above formulations; unfortunately, we have not been able to observe the resonance of the C_2 carbons in the ^{13}C NMR spectrum of **11**, which might enable a better comparison with related ligands to be made. As mentioned earlier, complex **11** is also relatively stable, probably because access to the C_2 unit is prevented by CO and Ph groups.

Reactions between $Ru_5(\mu_5\text{-}\eta^2,P\text{-}C_2PPh_2)(\mu\text{-}PPh_2)(CO)_{13}$ (2) and dihydrogen

We have found that two distinct types of reaction occur between **2** and dihydrogen, depending on the conditions. Partial degradation of the Ru_5 cluster occurs on treatment of **2** with H_2 under pressure (10 atm, 18 h) to give complex **12**, which contains a $HC{\equiv}CPPh_2$ ligand attached to an Ru-spiked triangular Ru_3 cluster by the P atom and a conventional $\mu_3\text{-}\eta^2(\|)$-alkyne interaction, as described earlier [11]. The fifth ruthenium carbonyl fragment is partially recovered as $Ru_4(\mu\text{-H})_4(CO)_{12}$. This reaction has been fully described elsewhere [10].

In contrast, passage of H_2 (1 atm) into a solution of **2** in refluxing cyclohexane cause the colour to lighten to red. Only traces of **12** and $Ru_4(\mu\text{-H})_4(CO)_{12}$ were obtained; preparative TLC enabled the separation of three major products, which were characterised as the black $Ru_5(\mu\text{-H})(\mu_5\text{-}C{=}CHPPh_2)(\mu\text{-}PPh_2)(CO)_{13}$ (**13**), the

Table 2. Core geometries for $Ru_5(\mu\text{-H})(\mu_5\text{-CCHPPh}_2)(\mu\text{-PPh}_2)(CO)_{13}$ (**13**) (r is the central–other atom distance (Å). Other entries in the matrices are the angles (degrees) subtended at the central atom by the other two atoms at the head of the relevant row and column)

Atom Ru(1)	r	Ru(5)	H(12)	P(1)	C(11)	C(12)	C(13)	
Ru(2)	3.0730(7)	54.54(1)	29.2(11)	88.59(3)	143.6(1)	86.7(1)	118.5(1)	
Ru(5)	2.9681(6)		82.8(11)	89.77(3)	89.3(1)	91.5(1)	173.0(1)	
H(12)	1.75(3)			80.2(12)	171.4(11)	93.3(12)	90.4(11)	
P(1)	2.388(1)				96.4(2)	173.2(1)	90.4(2)	
C(11)	1.909(5)					90.3(2)	97.6(2)	
C(12)	1.926(5)						87.6(2)	
C(13)	1.900(4)							
Atom Ru(2)	r	Ru(3)	Ru(5)	H(12)	P(2)	C(21)	C(22)	C(2)
Ru(1)	3.0730(7)	112.61(1)	60.80(2)	29.0(12)	153.67(4)	110.8(1)	89.5(1)	70.4(1)
Ru(3)	2.7805(7)		62.29(2)	127.2(11)	52.22(3)	106.6(1)	143.5(1)	46.0(1)
Ru(5)	2.7695(6)			88.7(11)	93.45(4)	156.2(1)	110.7(1)	50.1(1)
H(12)	1.77(3)				176.8(13)	82.1(12)	86.1(12)	81.4(11)
P(2)	2.326(1)					95.0(1)	95.3(1)	98.2(1)
C(21)	1.869(5)						90.7(2)	106.5(2)
C(22)	1.913(5)							157.0(2)
C(2)	2.175(4)							
Atom Ru(3)	r	Ru(4)	Ru(5)	P(2)	C(31)	C(32)	C(2)	
Ru(2)	2.7805(7)	99.74(2)	58.67(1)	53.59(3)	110.2(2)	151.5(2)	50.9(1)	
Ru(4)	2.8139(6)		59.93(2)	150.13(4)	98.4(1)	97.1(1)	50.6(1)	
Ru(5)	2.8705(8)			91.74(3)	149.6(1)	112.6(2)	48.8(1)	
P(2)	2.284(1)				103.5(1)	103.1(1)	104.5(1)	
C(31)	1.844(6)					89.7(2)	101.4(2)	
C(32)	1.895(5)						146.8(2)	
C(2)	2.014(3)							
Atom Ru(4)	r	Ru(5)	C(41)	C(42)	C(43)	C(1)	C(2)	
Ru(3)	2.8139(6)	61.02(2)	165.4(2)	96.2(1)	89.3(1)	77.14(8)	45.38(9)	
Ru(5)	2.8397(8)		104.4(2)	156.0(1)	93.6(2)	79.2(1)	48.9(1)	
C(41)	1.921(4)			98.1(2)	92.8(2)	100.1(2)	125.3(2)	
C(42)	1.895(6)				93.5(2)	88.8(2)	110.4(2)	
C(43)	1.929(5)					166.4(2)	129.1(2)	
C(1)	2.174(4)						38.4(7)	
C(2)	2.187(4)							
Atom Ru(5)	r	Ru(2)	Ru(3)	Ru(4)	C(51)	C(52)	C(53)	C(2)
Ru(1)	2.9681(6)	64.66(2)	113.13(2)	100.51(2)	90.0(1)	84.6(1)	171.9(2)	72.8(1)
Ru(2)	2.7695(6)		59.04(2)	99.37(2)	154.2(1)	81.8(1)	113.0(1)	50.5(1)
Ru(3)	2.8705(8)			59.04(1)	135.3(2)	118.0(1)	69.8(2)	44.5(1)
Ru(4)	2.8397(7)				80.1(2)	174.8(1)	87.5(2)	49.6(1)
C(51)	1.888(5)					101.1(2)	92.8(2)	120.0(2)
C(52)	1.910(5)						87.3(2)	132.1(2)
C(53)	1.893(4)							112.2(2)
C(2)	2.162(4)							
Atom C(2)	r	Ru(3)	Ru(4)	Ru(5)	C(1)			
Ru(2)	2.175(4)	83.1(1)	157.5(2)	79.4(1)	131.5(3)			
Ru(3)	2.014(3)		84.0(1)	86.8(1)	131.2(3)			
Ru(4)	2.187(4)			81.5(1)	70.3(2)			
Ru(5)	2.162(4)				127.2(3)			
C(1)	1.435(5)							

Also: C(1)–C(2), 1.435(5); C(1)–P(1), 1.788(4) Å
Ru(4)–C(1)–P(1), C(2), 124.7(2), 71.3(2);
P(1)–C(1)–C(2), 112.4(3)°
H(1)–C(1), 0.87(4)(Å); H(1)–C(1)–P(1), C(2), Ru(4), 113(2), 117(2), 112(2)°.

Table 3

Core geometries for $Ru_5(\mu\text{-}H)_2(\mu_4\text{-}CCH_2PPh_2)(\mu\text{-}PPh_2)(CO)_{12}$ (**14**) (r is the central atom–other atom distance (Å). Other entries in the matrices are the angles (degrees) subtended at the central atom by the relevant atoms at the head of the associated row and column.)

Atom Ru(1)	r	Ru(4)	Ru(5)	P(1)	C(11)	C(12)	C(2)
Ru(2)	2.771(2)	86.78(5)	60.63(4)	99.3(1)	150.6(4)	71.1(4)	50.6(3)
Ru(4)	2.871(2)		57.49(5)	88.8(1)	111.7(5)	157.8(4)	49.9(3)
Ru(5)	2.933(2)			139.5(1)	109.2(6)	109.9(5)	73.4(4)
P(1)	2.316(4)				103.6(5)	93.4(6)	67.3(4)
C(11)	1.89(1)					89.3(6)	157.7(8)
C(12)	1.86(1)						111.1(5)
C(2)	2.20(1)						
Atom Ru(2)	r	Ru(3)	Ru(5)	P(2)	C(21)	C(22)	C(2)
Ru(1)	2.771(2)	93.20(5)	62.46(5)	145.6(1)	103.1(4)	106.3(4)	51.2(3)
Ru(3)	2.683(2)		63.32(6)	54.2(1)	117.7(4)	142.8(5)	52.7(3)
Ru(5)	2.882(2)			89.9(1)	165.3(4)	97.8(5)	74.7(4)
P(2)	2.264(4)				102.4(4)	96.9(4)	104.3(3)
C(21)	1.89(2)					88.8(7)	94.3(6)
C(22)	1.91(1)						157.4(5)
C(2)	2.19(1)						
Atom Ru(3)	r	Ru(4)	Ru(5)	P(2)	C(31)	C(32)	C(2)
Ru(2)	2.683(2)	90.57(5)	61.66(5)	53.5(1)	108.6(4)	141.7(4)	52.0(3)
Ru(4)	2.771(2)		58.60(5)	141.2(1)	109.6(3)	113.9(4)	51.6(3)
Ru(5)	2.926(2)			88.3(1)	162.7(4)	105.3(5)	73.4(4)
P(2)	2.285(3)				96.9(4)	92.7(4)	102.9(3)
C(31)	1.90(2)					91.0(7)	89.3(5)
C(32)	1.92(2)						164.2(5)
C(2)	2.21(1)						
Atom Ru(4)	r	Ru(3)	Ru(5)	C(41)	C(42)	C(43)	C(2)
Ru(1)	2.871(2)	89.25(5)	62.37(4)	106.3(4)	115.9(5)	150.7(4)	49.3(3)
Ru(3)	2.771(2)		63.48(4)	122.2(4)	130.2(5)	61.5(4)	51.5(3)
Ru(5)	2.791(2)			168.2(4)	89.9(5)	102.7(5)	76.1(3)
C(41)	1.90(1)				92.6(7)	88.9(6)	99.3(6)
C(42)	1.90(2)					87.5(7)	163.2(6)
C(43)	1.95(1)						104.4(6)
C(2)	2.23(1)						
Atom Ru(5)	r	Ru(2)	Ru(3)	Ru(4)	C(51)	C(52)	C(53)
Ru(1)	2.933(2)	56.91(4)	85.15(5)	60.15(6)	116.4(6)	146.7(5)	91.5(6)
Ru(2)	2.882(2)		55.02(5)	86.17(6)	83.5(6)	124.9(5)	142.9(6)
Ru(3)	2.926(2)			57.92(4)	112.3(4)	75.3(6)	149.8(5)
Ru(4)	2.791(2)				168.9(5)	86.6(5)	94.5(5)
C(51)	1.92(1)					96.1(7)	96.1(6)
C(52)	1.89(2)						92.2(8)
C(53)	1.91(2)						
Atom C(2)	r	Ru(2)	Ru(3)	Ru(4)	C(1)		
Ru(1)	2.20(1)	78.2(4)	127.8(7)	80.8(5)	105.7(8)		
Ru(2)	2.19(1)		75.2(4)	122.9(7)	119.2(9)		
Ru(3)	2.21(1)			77.4(5)	126.5(9)		
Ru(4)	2.23(1)				117.5(7)		
C(1)	1.39(2)						

Also: C(1)–P(1), 1.88(2) Å, P(1)–C(1)–C(2), 99(1)°

dark red $Ru_5(\mu\text{-}H)_2(\mu_4\text{-}CCH_2PPh_2)(\mu\text{-}PPh_2)(CO)_{12}$ (**14**), and the orange $Ru_5C(\mu\text{-}H)_3(\mu\text{-}PPh_2)(CO)_{11}(PMePh_2)$ (**15**) by X-ray crystallographic studies (Tables 1–8). The relative amounts of the three complexes depend on the time of reaction, and we have shown that it is possible to convert **13** into **14** and **15**, and **14** into **15**, by further reaction with H_2 under similar conditions. The three complexes thus provide an unusual opportunity to examine in detail the course of the reaction of H_2 with a

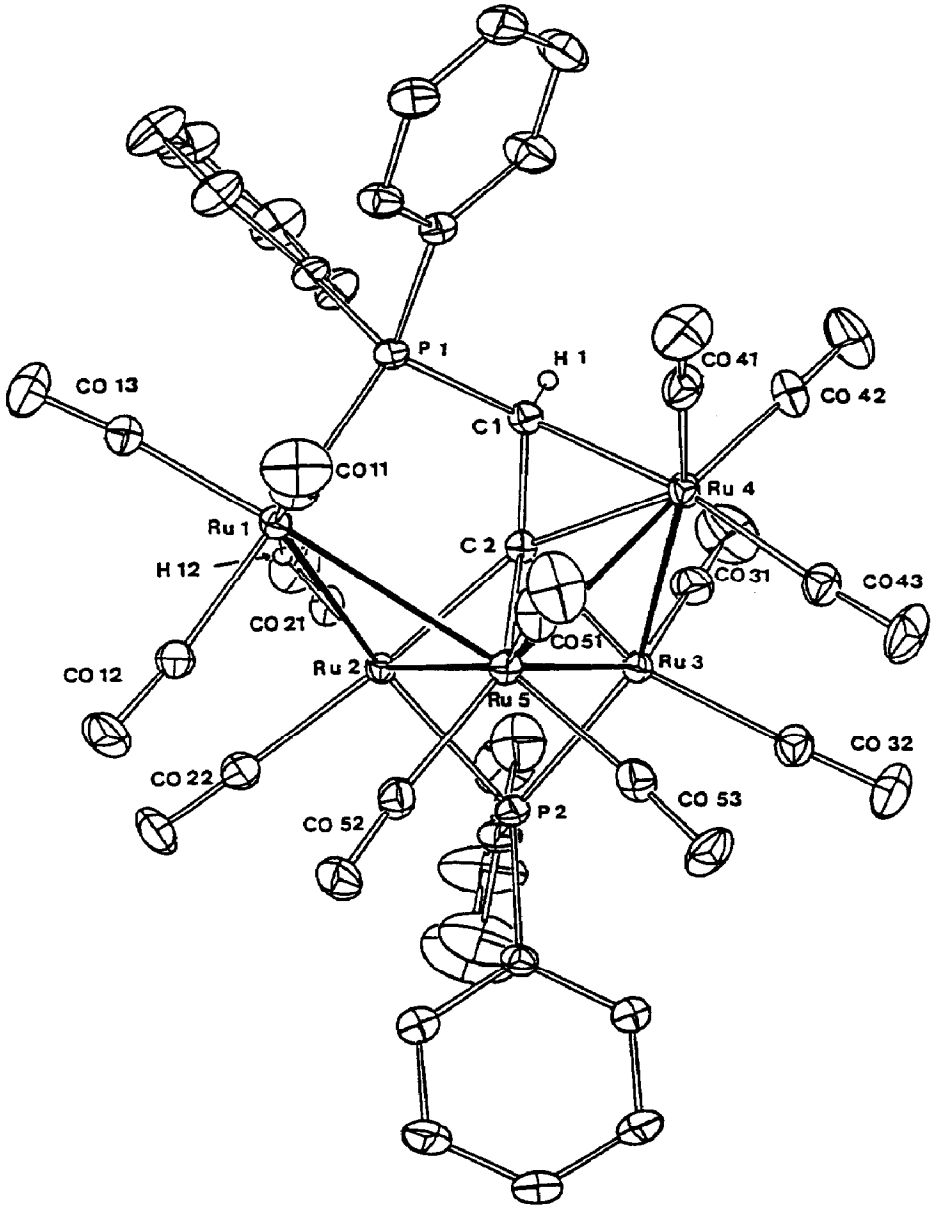

Fig. 1. Plot of a molecule of $Ru_5(\mu\text{-}H)(\mu_5\text{-}CCHPPh_2)(\mu\text{-}PPh_2)(CO)_{13}$ (**13**), showing core atom labelling scheme. (N.B. This scheme does not correspond with that given in ref. 12). Non-hydrogen atoms shown as 20% thermal ellipsoids; hydrogen atoms have arbitrary radii of 0.1 Å.

Table 4

Core geometries for $Ru_5C(\mu\text{-}H)_3(\mu\text{-}PPh_2)(CO)_{11}(PMePh_2)$ (**15**) (r is the central–other atom distance (Å). Other entries in the matrices are the angles (degrees), subtended at the central atom by the relevant atoms at the head of the associated row and column)

Atom Ru(1)	r	Ru(3)	Ru(4)	Ru(5)	H(12)	H(14)	H(15)	P(1)	C(11)	C(2)
Ru(2)	2.8347(5)	58.97(2)	93.05(1)	61.22(2)	41(1)	134(1)	86(1)	130.30(2)	109.25(8)	46.63(6)
Ru(3)	2.8820(6)		60.79(1)	87.46(1)	87(1)	90(1)	123(1)	166.46(3)	75.82(5)	43.15(8)
Ru(4)	2.8391(6)			60.80(2)	133(1)	41(1)	81(1)	123.81(2)	108.49(9)	46.43(6)
Ru(5)	2.8934(6)				87(1)	88(1)	36(1)	105.91(2)	163.24(8)	44.33(8)
H(12)	1.73(3)					175(2)	92(2)	96(1)	93(2)	87(1)
H(14)	1.72(3)						86(2)	88(1)	90(1)	88(1)
H(15)	1.77(5)							70(1)	161(1)	80(1)
P(1)	2.3408(8)								90.75(8)	150.09(9)
C(11)	1.863(4)									118.9(1)
C(2)	2.075(2)									

Atom Ru(2)	r	Ru(3)	Ru(5)	H(12)	P(2)	C(21)	C(22)	C(2)
Ru(1)	2.8347(5)	61.88(2)	60.38(2)	36(1)	93.57(2)	149.17(9)	113.33(8)	46.93(6)
Ru(3)	2.7705(6)		89.13(1)	87(1)	53.00(2)	104.12(8)	155.1(1)	45.26(8)
Ru(5)	2.9170(6)			84(1)	141.94(1)	94.1(1)	110.1(1)	43.87(8)
H(12)	1.88(3)				91(1)	168(1)	79(1)	83(1)
P(2)	2.309(1)					98.6(1)	105.5(1)	98.16(9)
C(21)	1.865(3)						90.6(1)	103.0(1)
C(22)	1.904(3)							150.6(1)
C(2)	2.065(2)							

Atom Ru(3)	r	Ru(2)	Ru(4)	P(2)	C(31)	C(32)	C(2)
Ru(1)	2.8820(6)	60.16(1)	58.87(2)	92.46(2)	155.5(1)	107.97(8)	46.04(6)
Ru(2)	2.7705(6)		93.20(1)	53.18(2)	109.70(9)	149.6(1)	48.07(6)
Ru(4)	2.8948(6)			145.25(2)	102.4(1)	104.0(1)	45.35(6)
P(2)	2.3040(7)				97.98(9)	103.5(1)	101.14(7)
C(31)	1.871(3)					91.1(1)	109.9(1)
C(32)	1.923(4)						144.9(1)
C(2)	1.971(3)						

Atom Ru(4)	r	Ru(3)	Ru(5)	H(14)	C(41)	C(42)	C(43)	C(2)
Ru(1)	2.8391(6)	60.34(1)	60.522(8)	36(1)	110.85(9)	143.63(8)	108.4(1)	46.85(6)
Ru(3)	2.8948(6)		87.07(1)	86(1)	167.8(1)	94.8(1)	81.5(1)	42.89(8)
Ru(5)	2.9014(7)			85(1)	95.6(1)	94.5(1)	167.2(1)	44.18(9)
H(14)	1.92(3)				83(1)	179(1)	89(1)	83(1)
C(41)	1.928(3)					96.7(1)	94.4(1)	138.4(1)
C(42)	1.911(3)						92.1(1)	96.8(1)
C(43)	1.907(4)							124.1(1)
C(2)	2.060(2)							

Atom Ru(5)	r	Ru(20	Ru(4)	H(15)	C(51)	C(52)	C(53)	C(2)
Ru(1)	2.8934(6)	58.40(2)	58.67(2)	35(1)	114.4(1)	105.8(1)	142.7(1)	45.81(6)
Ru(2)	2.9170(6)		90.09(1)	84(1)	171.71(9)	80.6(1)	95.2(1)	45.04(6)
Ru(4)	2.9014(7)			79(1)	88.9(1)	164.5(1)	99.5(1)	45.24(6)
H(15)	1.79(3)				88(1)	87(1)	178(1)	81(1)
C(51)	1.947(4)					98.5(1)	93.1(2)	134.1(1)
C(52)	1.919(3)						93.8(1)	125.2(1)
C(53)	1.921(3)							97.0(1)
C(2)	2.022(3)							

Atom C(2)	r	Ru(2)	Ru(3)	Ru(4)	Ru(5)
Ru(1)	2.075(2)	86.4(1)	90.8(1)	86.7(1)	89.9(1)
Ru(2)	2.065(2)		86.7(1)	173.0(1)	91.1(1)
Ru(3)	1.971(3)			91.8(1)	177.6(1)
Ru(4)	2.060(2)				90.6(1)
Ru(5)	2.022(3)				

Table 5

Carbonyl geometries for $Ru_5(\mu\text{-H})(\mu_5\text{-CCHPPh}_2)(\mu\text{-PPh}_2)(CO)_{13}$ (13)

Carbonyl, *lm*	*r*(Ru(*l*)–C) (Å)	*r*(C–O) (Å)	Angle Ru–C–O (°)
11	1.909(5)	1.142(6)	175.3(5)
12	1.926(5)	1.140(6)	174.0(4)
13	1.900(4)	1.120(6)	174.1(5)
21	1.869(5)	1.136(6)	178.0(3)
22	1.913(5)	1.129(6)	177.1(4)
31	1.844(6)	1.140(7)	178.9(4)
32	1.895(5)	1.152(6)	178.3(4)
41	1.921(4)	1.126(6)	176.8(5)
42	1.895(6)	1.129(8)	176.5(4)
43	1.929(5)	1.130(6)	175.8(5)
51	1.888(5)	1.156(6)	175.2(5)
52	1.910(5)	1.140(7)	174.9(4)
53	1.893(4)	1.150(6)	170.6(5)

Table 6

Carbonyl geometries for $Ru_5(\mu\text{-H})_2(\mu_4\text{-CCH}_2\text{PPh}_2)(\mu\text{-PPh}_2)(CO)_{12}$ (14)

Carbonyl, *lm*	*r*(Ru(*l*)–C) (Å)	*r*(C–O) (Å)	Angle Ru–C–O (°)
11	1.89(1)	1.15(2)	177(2)
12	1.85(2)	1.16(2)	172(1)
21	1.89(2)	1.14(2)	176(1)
22	1.91(1)	1.12(2)	178(1)
31	1.90(2)	1.12(2)	176(1)
32	1.92(2)	1.13(2)	177(1)
41	1.90(1)	1.15(2)	173(1)
42	1.90(2)	1.14(2)	179(1)
43 [a]	1.95(1)	1.15(2)	159(1)
51	1.92(1)	1.16(2)	175(2)
52	1.89(2)	1.14(2)	173(1)
53	1.91(2)	1.14(2)	177(2)

[a] Ru(3)–C(43), 2.51(1) Å; Ru(3)–C(43)–O(43), Ru(4), 126(1), 75.6(5)°.

Table 7

Carbonyl geometries for $Ru_5C(\mu\text{-H})_3(\mu\text{-PPh}_2)(CO)_{11}(PMePh_2)$ (15)

Carbonyl, *lm*	*r*(Ru(*l*)–C) (Å)	*r*(C–O) (Å)	Angle Ru–C–O (°)
11	1.863(4)	1.151(5)	173.0(2)
21	1.865(3)	1.139(3)	176.2(3)
22	1.904(3)	1.128(4)	179.4(3)
31	1.871(3)	1.133(4)	176.6(4)
32	1.923(4)	1.130(5)	179.1(3)
41	1.928(3)	1.132(4)	176.9(3)
42	1.911(3)	1.129(4)	177.8(3)
43	1.907(4)	1.129(4)	175.3(3)
51	1.946(4)	1.123(5)	177.2(3)
52	1.919(3)	1.138(4)	176.6(2)
53	1.921(3)	1.124(4)	178.5(3)

Table 8

Phosphorus geometries for **13**, **14**, **15**

n	(13)		(14)		(15)	
	1	2	1	2	1	2
Distances (Å)						
P(*n*)–C(*n*11)	1.829(5)	1.826(5)	1.83(2)	1.84(1)	1.831(3)	1.825(3)
P(*n*)–C(*n*21)	1.821(4)	1.826(4)	1.80(1)	1.83(2)	1.818(3)	1.827(2)
P(*n*)–C(1)	1.788(4)	(2.284(1))	1.88(1)	(2.285(3))	1.825(5)	(2.3040(7))
Angles (degrees)						
Ru(*n*)–P(*n*)–C(*n*11) [a]	111.6(1)	120.6(1)	121.2(4)	122.6(5)	118.51(8)	120.6(1)
Ru(*n*)–P(*n*)–C(*n*21)	124.4(2)	117.5(1)	122.7(5)	118.9(4)	112.40(8)	119.4(1)
Ru(*n*)–P(*n*)–C(1)	104.9(1)	–	86.9(6)	–	116.81(8)	–
C(*n*11)–P(*n*)–C(*n*21)	100.1(2)	102.6(2)	100.7(6)	100.5(6)	100.9(1)	102.5(1)
C(*n*11)–P(*n*)–C(1) [b]	105.1(2)	(119.1(1))	110.9(6)	(118.9(4))	101.8(2)	(117.7(1))
C(*n*21)–P(*n*)–C(1) [b]	109.4(2)	(122.3(2))	114.1(6)	(124.0(5))	104.2(1)	(122.4(1))
Ru(*n*)–P(2)–Ru(3)	–	74.18(3)	–	72.3(1)	–	73.81(3)

[a] For $n = 2$, read (Ru(3)–P(2)). [b] For $n = 2$, read (C(211,221)–P(2)–Ru(3)).

cluster-bound ethynyl ligand, during which stepwise addition of up to three molecules of H_2 to **2** occurs.

We present here a fuller discussion of the molecular structures of **13** and **15** than was possible in the original communication, together with a description of the molecular structure of **14**, which differs from that previously proposed [12]. Figures 1–3 are plots of the structures of **13**, **14** and **15**, respectively, while Scheme 2 summarises the reactions.

The ^{1}H NMR spectrum of complex **13**, which was also obtained in 24% yield by successive addition of H^- (as $K[BHBu^s_3]$) and H^+ (as H_3PO_4) to **2**, contains three resonances. That at δ 7.42 was readily assigned to the Ph protons, and one at δ −13.1 to a proton bridging two rutheniums and coupled to two inequivalent phosphorus atoms. A doublet at δ 5.86 is consistent with the CH of a vinylidene coupled to phosphorus; similar resonances have been reported at δ 5.10 in $Ru_3(\mu\text{-}H)(\mu_3\text{-}CCHPr^i)(\mu\text{-}PPh_2)(CO)_8$ [6], and at δ 6.30 in $Au_2Ru_3(\mu_3\text{-}CCHBu^t)(CO)_9(PPh_3)_2$ [27].

The Ru_5 core in **13** is essentially unchanged from that in **2**, although a hydrogen atom bridges the Ru(1)–Ru(2) bond (Fig. 1). A second hydrogen atom has become attached to the β-carbon of the ethynyl group, forming a μ_5-η^2,*P*-diphenylphosphinovinylidene ligand, bonded to Ru(1) by the P(1) atom (Ru(1)–P(1) 2.388(1) Å), to Ru(2), Ru(3) and Ru(5) via C(2) only (Ru(2)–C(2) 2.175(4), Ru(3)–C(2) 2.014(3), Ru(5)–C(2) 2.162(4) Å), and to Ru(4) by both carbon atoms (Ru(4)–C(1) 2.174(4), Ru(4)–C(2) 2.187(4) Å). The site of the cluster-bonded H atom is indicated by the usual lengthening of the bridged Ru–Ru vector (Ru(1)–Ru(2) 3.0730(7) Å), and by the splaying out of the CO groups attached to these metal atoms. Compared with **2**, addition of hydrogen to the β-carbon has resulted in the α-carbon being further removed from Ru(2), (ca. 0.15 Å) whilst the Ru(3)–C(2) separation remains essentially unchanged.

Addition of another molecule of H_2 to **13** resulted in the formation of **14** in 25–30% yield, containing a diphenylphosphinomethylmethylidyne ligand, the α-

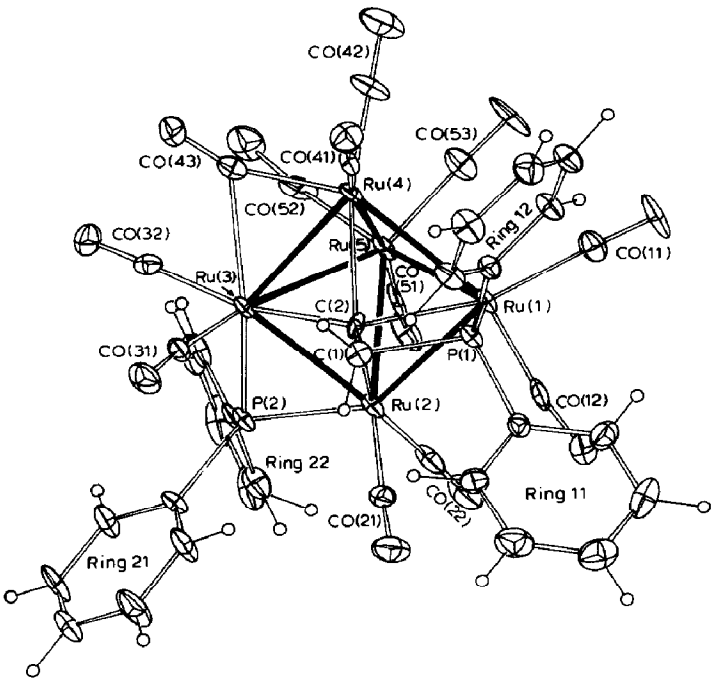

Fig. 2. Plot of a molecule of $Ru_5(\mu\text{-}H)_2(\mu_4\text{-}CCH_2PPh_2)(\mu\text{-}PPh_2)(CO)_{12}$ (**14**), showing core atom labelling scheme. Non-hydrogen atoms shown as 20% thermal ellipsoids; hydrogen atoms have arbitrary radii of 0.1 Å.

carbon of which interacts with four Ru atoms in the square face of a square pyramidal Ru_5 cluster in **14**. Alternatively, the cluster can be regarded as a derivative of the Ru_4C cluster, bearing an alkylated carbido carbon. The ^1H NMR spectrum contains a two-proton multiplet at δ 5.04 for the CH_2 group, and at high field, a doublet of doublets at δ −20.2 for the two μ-H ligands coupled to inequivalent phosphorus atoms.

Complex **14** (Fig. 2) consists of a nearly square pyramid of five ruthenium atoms, one edge of which is bridged by the PPh_2 group (Ru(2)–Ru(3) 2.683(2), Ru(2)–P(2) 2.264(4), Ru(3)–P(2) 2.285(3) Å) and an adjacent edge by a semi-bridging CO ligand (Ru(3)–Ru(4) 2.771(2), Ru(3)–C(43) 2.51(1), Ru(4)–C(43) 1.95(1) Å; Ru(3)–C(43)–O(43) 126(1)°). The apical ruthenium is not equidistant from the other four ruthenium atoms, the longer Ru(1)–Ru(5) (2.933(2) Å) and Ru(3)–Ru(5) (2.926(2) Å) distances suggesting that the two metal-bonded H atoms bridge these edges. The methylidyne carbon is equidistant from the four Ru atoms in the square face (Ru(1)–C(2) 2.20(1), Ru(2)–C(2) 2.19(1), Ru(3)–C(2) 2.21(1), Ru(4)–C(2) 2.23(1) Å), although these distances are ca. 0.2 Å longer than those found in $Ru_5C(CO)_{15}$ (av. 2.02 Å) [28]. It is also bonded to the methylene group by a short C–C bond (C(1)–C(2) 1.39(2) Å), and the second PPh_2 group is attached to Ru(1) by a normal 2e donor bond (Ru(1)–P(2) 2.316(4) Å).

Although μ_3-CR ligands have been known since the discovery of $Co_3(\mu_3\text{-}CR)(CO)_9$ complexes [29], and have featured in the chemistry of heterometallic clusters derived from tungsten carbyne and related complexes [30], there is only one previous example of a compound containing a μ_4-CR ligand spanning a square M_4 face, namely $Pt_2Ru_2(\mu\text{-}H)(\mu_4\text{-}CH)(\mu\text{-}CO)(CO)_2(PPr^i_3)_2(\eta\text{-}C_5H_5)_2$ [31]. In $Fe_4(\mu$-

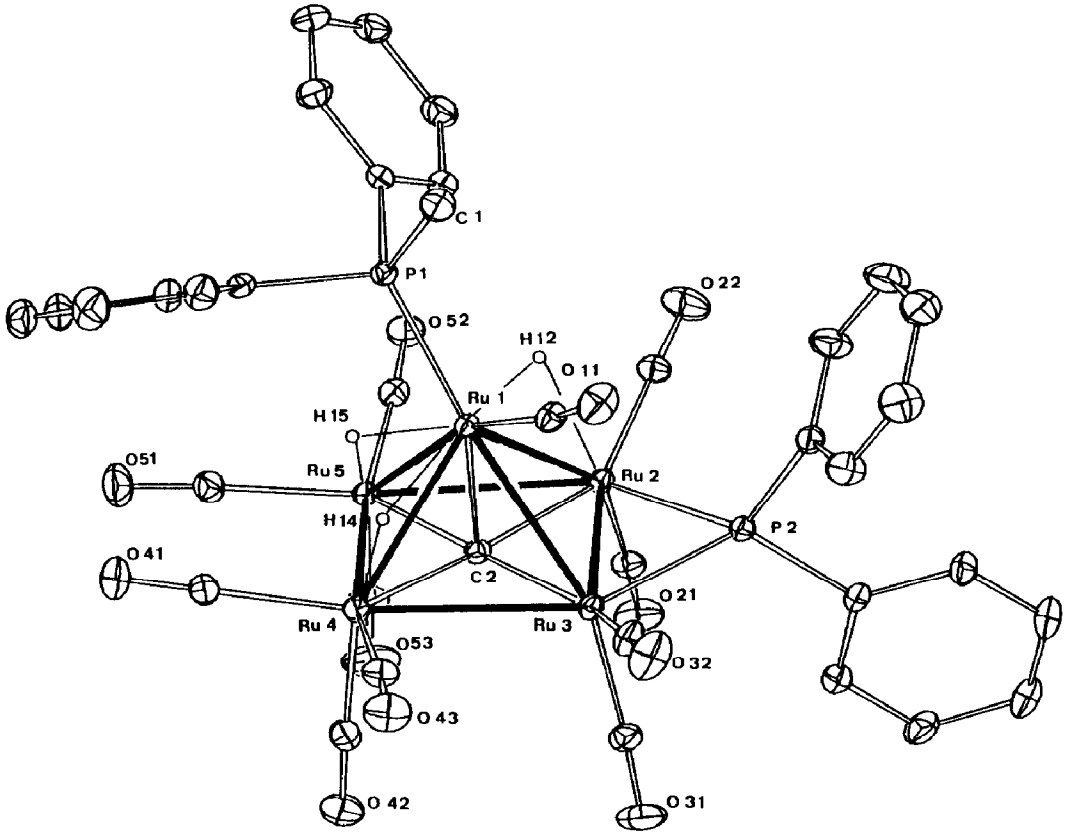

Fig. 3. Plot of a molecule of $Ru_5C(\mu\text{-}H)_3(\mu\text{-}PPh_2)(CO)_{11}(PMePh_2)$ (**15**), showing core atom labelling scheme. (N.B. This scheme does not correspond with that given in ref. 12). Non-hydrogen atoms shown as 20% thermal ellipsoids; hydrogen atoms have arbitrary radii of 0.1 Å.

$H)(\mu_4\text{-}CH)(CO)_{12}$, the metal skeleton has a bufferfly configuration, and the methine hydrogen shows an agostic interaction with a wing-tip Fe atom [32]. Several related complexes derived from $[Fe(\mu_4\text{-}C)(CO)_{12}]^{2-}$ have also been described [7].

Complex **14** is readily converted into the trihydrido cluster **15** in 30–55% yield by addition of a further molecule of H_2. The resulting complex is formed by cleavage of the μ_4-C–CH_2 bond in **14**, and is a derivative of the well-known cluster $Ru_5C(CO)_{15}$. The ^1H NMR spectrum contains a characteristic three-proton doublet at δ 1.88 for the Me group of the $PMePh_2$ ligand, together with two high-field multiplets at δ −19.97 and −22.50 (relative intensity 2/1) for the three μ-H atoms.

In **15**, the distorted square-pyramidal Ru_5C cluster (C(2) lies 0.06 Å below the average plane of the square base) contains three μ-H atoms, eleven terminal CO groups, the $PMePh_2$ ligand and the μ-PPh_2 group (Fig. 3). The hydrogen atoms bridge three of the Ru(1)–Ru(basal) bonds; unexpectedly, no lengthening of these bonds (av. 2.856 Å) over the remaining unbridged bond (2.882(1) Å) is found. In contrast, the basal Ru–Ru separations are generally longer (2.8948(7)–2.9170(6) Å) except for Ru(2)–Ru(3) (2.7705(6) Å), which is bridged by the PPh_2 group. The Ru–C(carbide) distances (mean 2.04(1) Å) are not significantly different from those in $Ru_5C(CO)_{15}$ (mean 2.02(2) Å) [28].

Complex **15** is the first derivative of $Ru_5C(CO)_{15}$ containing a μ-PR_2 group; it is also noteworthy that the $PMePh_2$ ligand is located on the apical metal atom, whereas normal CO-substitution reactions afford derivatives in which the tertiary phosphines occupy axial sites on basal ruthenium atoms [28].

Discussion

The skeletal changes occurring in the reactions between **2** and CO are shown in Scheme 2. Complexes **9** and **10** are both 80e five-atom clusters, the transformation from the swallow cluster (or three edge-fused triangles) to the M_2-spiked triangle occurring by breaking of two Ru–Ru bonds. The swallow cluster itself can be obtained by breaking one Ru–Ru bond of a square pyramidal Ru_5 core, as found when $Ru_5(\mu_4\text{-}C_2Ph)(\mu\text{-}PPh_2)(CO)_{13}$ (**6**) reacts with CO to give **7**; an alternative reaction, with $PHPh_2$, gave the bow-tie cluster present in $Ru_5(\mu\text{-}H)(\mu_4\text{-}C_2Ph)(\mu\text{-}PPh_2)_2(CO)_{13}$ (**17**) by addition of the 4e ligand set ($H + PPh_2$). The bridging C_2PPh_2 ligand in **2** plays a pivotal role in preventing condensation of the Ru_5 cluster in the reactions discussed in this paper.

We have shown that the novel isomerisation **9** → **10** occurs in the presence of CO, and have suggested that the reaction proceeds by addition and elimination of CO; unfortunately, we have not been able to carry out any labelling experiment to substantiate this hypothesis. Although **8** readily reverts to **2** by loss of CO, this transformation is more difficult with the isomeric complex **10**.

Excission of one of the rutheniums occurs under more vigorous conditions, with concomitant cleavage of a P–C(*sp*) bond, to give **11**. The route to this unusual complex is not clear, but is undoubtedly related to that which generates **4**, a complex isolated from the thermal reaction between dppa and $Ru_3(CO)_{12}$ [3]. Interestingly, the lengthening of the C–C bond in **11** to 1.275 Å parallels that found in the first excited level of free C_2 (1.26 Å).

The ability of the C_2PPh_2 ligand to preserve an open cluster is also seen in the reactions with dihydrogen. Under vigorous conditions loss of one of the rutheniums (presumably as $HRu(CO)_3$, which is recovered as $Ru_4(\mu\text{-}H)_4(CO)_{12}$), affords the Ru-spiked triangular cluster found in **12**. The tertiary phosphine is coordinated to the 'outside' Ru, while the PPh_2 group unusually bridges two non-bonded metal atoms. The alkyne function interacts with the triangular Ru_3 unit in the normal way, and it is tempting to argue that the geometry of the ethynylphosphine prevents isomerisation to the vinylidene often found with similar complexes, such as $Co_2Ru(\mu_3\text{-}HC_2Bu^t)(CO)_9$ [33]. However, this isomerisation is thought to proceed by addition of the H–C≡C across a M–M bond to give a hydrido-acetylide cluster, hydrogen transfer to the β-carbon from the cluster then generating the vinylidene. We note that in **12** all the Ru–Ru bonds of the Ru_3 triangle are already bridged by μ-H atoms, which may also be a factor preventing the isomerisation reaction.

The stepwise transformation of **2** to **13**, **14** and **15** which occurs under milder conditions shows that preservation of the open Ru_5 cluster, facilitated by the ethynylphosphine ligand, allows addition of dihydrogen to both the cluster and the C_2 group. Complex **13** was initially made by successive addition of H^- and H^+ to **2**; it is likely that attack on the β-carbon by H^- is followed by addition of H^+ to the cluster. The reaction of **2** with H_2 is facile and a striking illustration of the increased reactivity of the C_2 unit when attached to four metal atoms.

The subsequent reactions are promoted by Ru–Ru bond formation and incorporation of the α-carbon into the square face of the square-pyramidal Ru_5 cluster so formed. The ready cleavage of the C–C bond in **14** upon reaction with H_2 is an indication of the stability of the Ru_5C core, in agreement with other attempts to induce the carbido carbon in $Ru_5C(CO)_{15}$ to enter into reaction. As depicted in Scheme 2, the conversions follow an easily recognisable path, since **2** forms **13** and then **14**, with bond formation between Ru(1) and Ru(4); some rearrangements of ligands, e.g. formation of a μ-CO group, and migration of H atoms, also ensue. In **15**, however, although the Ru_5C skeleton is preserved, P(1) is located on the apical Ru(1), while the PPh_2 group bridges a basal edge as in **14**. The simplest rationalisation of this process involves addition of one hydrogen to the cluster and one hydrogen to C(2); the resulting cleavage of the C(1)–C(2) bond is accompanied by formation of a bond C(1)–Ru(5) and migration of the new $PMePh_2$ ligand from Ru(1) to Ru(5) (Note that Ru(1) and Ru(5) in **14** become Ru(5) and Ru(1), respectively, in **15**). Migration of a tertiary phosphine is a process only recently observed unambiguously for the first time in the coordinatively unsaturated platinum clusters $[Pt_3(\mu_2\text{-CO})(\mu\text{-dppm})_3(L)]^{2+}$ (L = $P(OMe)_3$, $P(OEt)_3$, $P(OPh)_3$, PMe_2Ph) [34]. An alternative sequence, after cleavage of the C(1)–C(2) bond, is insertion of C(2) into Ru(3)–Ru(5), followed by formation of the Ru(1)–Ru(3) bond (Note in this sequence, the numerical identities of the Ru atoms are preserved).

The overall course of the reaction of **2** with dihydrogen is surprising: the C≡C bond is converted into C + CH_3, the former being incorporated into the cluster, and the methyl group appearing as the familiar ligand $PMePh_2$:

$$[\overline{Ru_5}]\text{–}C{\equiv}C\overline{P}Ph_2 \xrightarrow{2H} [H\overline{Ru_5}]{=}C{=}CH\overline{P}Ph_2 \xrightarrow{2H} \left[H_2\overline{Ru_5}\right]{\equiv}C\text{–}CH_2\overline{P}Ph_2 \xrightarrow{2H}$$

$$[H_3\overline{Ru_5C}]\quad Me\overline{P}Ph_2$$

The difference in behaviour between CO and H_2, both nominally 2e donors, can be explained by the requirement of 1e from the cluster for each C–H and Ru–H bond formed, so that all four complex **2**, **13**, **14** and **15** are 74e systems.

The normal course of hydrogenation of a C≡C triple bond is initial *cis* addition and eventual formation of the corresponding alkane. We note that this is the reaction pattern found for addition of H_2 to $Ru_3(\mu\text{-H})(\mu_3\text{-}C_2Bu^t)(CO)_9$ [35] and for

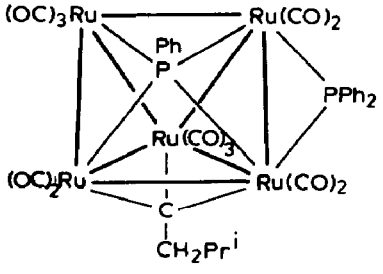

(18)

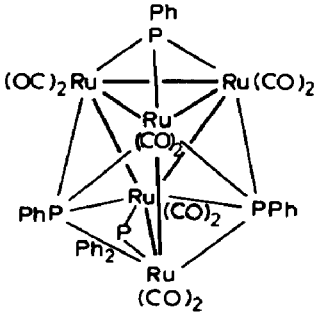

(19)

6 ($R = Pr^i$) in its reaction with PH_2Ph [36]. The former reaction gave $H_2Ru_3(\mu_3\text{-}CCH_2Bu^t)(CO)_9$, while the latter afforded $Ru_5(\mu_4\text{-}PPh)(\mu_3\text{-}CCH_2Pr^i)(\mu\text{-}PPh_2)(CO)_{12}$ (**18**) and $Ru_5(\mu_3\text{-}H)(\mu_4\text{-}PPh)_2(\mu_3\text{-}PPh)(CO)_{10}$ (**19**), which was also formed from **17** and PH_2Ph. In contrast, hydrogenation of **2** results in cleavage of the C≡C bond, a reaction driven by the formation of a new metal–metal bonds and a stable carbido cluster.

Similar considerations the account for the occurrence of the formal reaction. $2CO \rightarrow C + CO_2$ in the formation of $Ru_6C(CO)_{17}$ from $Ru_3(CO)_{12}$ at 170 °C [37], and of the formal reaction $Bu^tNC + CO \rightarrow C + Bu^tNCO$ in the pyrolysis of $Ru_5(\mu_5\text{-}CNBu^t)(CO)_{14}(CNBu^t)$ (which has an Ru_5 skeleton related to that in **2** [38]) to $Ru_6C(CO)_{16}(CNBu^t)$ [39].

Reductive transformations of ethyne to methane, and of phenylethyne to toluene and CO, have been achieved by use of mononuclear ammineruthenium(II) complexes; in the former case, it was considered likely that a first-formed σ-ethynyl complex was successively transformed into vinylidene, carbene, and alkyl complexes before the final addition of hydrogen and concomitant C–C breaking occurred [40].

Conclusion

We observed two types of reactions found for the open Ru_5 cluster in **2**. In the first, addition of 2e donor ligands (CO) results in the cleavage of Ru–Ru bonds, while the C_2PPh_2 ligand prevents degradation of the cluster. Addition of dihydrogen, on the other hand, occurs to both the cluster and the C_2 fragment, with a progressive tightening of the attachment of the α-carbon to the cluster, this atom finally being incorporated as carbide into the core. It is only under more vigorous conditions that some loss of metal occurs to give well-characterised open tetranuclear complexes.

Our studies have further demonstrated the remarkable reactivity of small molecules in open cluster systems, and the role played by the multi-metal attachment of unsaturated species in directing their reactions along paths quite different from those found for the free molecules or in mononuclear systems.

Experimental

General experimental conditions

All reactions were carried out under nitrogen unless otherwise stated. Common organic solvents were dried and distilled under nitrogen. Light petroleum refers to a fraction of b.p. 62–65 °C. $Ru_3(CO)_{12}$ [41] and sodium diphenyl ketyl solutions [42] were prepared by published procedures. Reagents were commercial products and were used as received. High purity nitrogen and hydrogen were obtained from Commonwealth Industrial Gases (CIG, Ltd.) and carbon monoxide from Matheson Gas Products; gases were used as received. High pressure reactions were carried out in a Roth stainless steel autoclave, internal volume 100 ml, equipped with a removable glass liner. Thin layer chromatography (TLC) was carried out on preparative plates (20 × 20 cm) coated with Kieselgel 60 GF_{254}. Elemental microanalyses were determined by the Canadian Microanalytical Service (Vancouver).

Instrumentation. Infrared spectra were recorded (by use of sodium chloride solution cells) on a Perkin–Elmer 683 double beam infrared spectrophotometer

calibrated with CO gas (2147.1 cm^{-1}). NMR spectra were recorded on Bruker WP-80DS (^1H, 80 MHz; ^{13}C, 20.1 MHz) or CXP300 (^1H, 300 MHz; ^{13}C, 75.37 MHz) spectrometers. Deuterated solvents were required for the deuterium resonance lock and were used in 2.5, 5 or 10 mm tubes. Shifts are reported relative to internal $SiMe_4$ (^1H, ^{13}C).

Reactions of $Ru_5(\mu_5\text{-}\eta^2,P\text{-}C_2PPh_2)(\mu\text{-}PPh_2)(CO)_{13}$ (2) with CO

A. Synthesis of $Ru_5(\mu_5\text{-}\eta^2,P\text{-}C_2PPh_2)(\mu\text{-}PPh_2)(CO)_{15}$ ('kinetic' isomer, 9). (i) A solution of **2** (90 mg, 0.071 mmol) in cyclohexane (50 cm^3) was carbonylated in an autoclave (10 atm, 25 °C, 36 h). The resulting red precipitate was filtered off, washed with cyclohexane (2 × 5 cm^3) and dried to give $Ru_5(\mu_5\text{-}\eta^2,P\text{-}C_2PPh_2)(\mu\text{-}PPh_2)(CO)_{15}$ (**9**) (79 mg, 84%), m.p. 141–143 °C (dec). (Found: C, 37.26; H, 1.26. $C_{41}H_{20}O_{15}P_2Ru_5$ calc.: C, 37.31; H, 1.53%). IR (cyclohexane): ν(CO) 2112m, 2074m, 2060(sh), 2053s, 2044s, 2036(sh), 2018m, 2002s, 1987w, 1965w, 1954w cm^{-1}.

(ii) Carbon monoxide was passed through a solution of **2** (80 mg, 0.063 mmol) in cyclohexane (40 ml) for 6 h to give **9** as a red precipitate (66 mg, 79%), identified by comparison of its IR ν(CO) spectrum with that of the sample prepared above.

B. Synthesis of $Ru_5(\mu_5\text{-}\eta^2,P\text{-}C_2PPh_2)(\mu\text{-}PPh_2)(CO)_{15}$ ('thermodynamic' isomer, 10). Carbon monoxide was passed through a solution of **2** (150 mg, 0.119 mmol) in cyclohexane (70 ml) at 70 °C for 18 h. Evaporation and preparative TLC (light petroleum/acetone 85/15) gave two bands: Band 1, R_f 0.40, black, recrystallized from CH_2Cl_2/MeOH to give black crystals of **2** (21 mg, 14%), identified by its infrared spectrum. Band 2, R_f 0.10, red, recrystallized from CH_2Cl_2/MeOH under a CO atmosphere to give red crystals of $Ru_5(\mu_5\text{-}\eta^2,P\text{-}C_2PPh_2)(\mu\text{-}PPh_2)(CO)_{15}$ (**10**) (55 mg, 35%), m.p. 160–163 °C (dec.). (Found: C, 37.19; H, 1.56; $C_{41}H_{20}O_{15}P_2Ru_5$ calc.: C, 37.31; H, 1.53%). IR (cyclohexane): ν(CO) 2100w, 2071w, 2067(sh), 2040s, 2037(sh), 2009w, 1999m, 1990w, 1983w, 1973w, 1966w cm^{-1}. ^1H NMR: δ ($CDCl_3$) 7.15 (m, Ph).

C. Synthesis of $Ru_4(\mu_4\text{-}C_2)(\mu\text{-}PPh_2)_2(CO)_{12}$ (11). A solution of (**2**) (80 mg, 0.06 mmol) in cyclohexane (40 ml) was carbonylated in an autoclave (20 atm, 100 °C, 16 h). The resulting yellow solution was evaporated to dryness and the residue subjected to preparative TLC (light petroleum/acetone 95/5) to give two major products. Band 1 (R_f 0.48) gave orange $Ru_3(CO)_{12}$ (20 mg) identified by comparison of its IR ν(CO) spectrum with that of an authentic sample. Band 2 (R_f 0.35), yellow, was recrystallized (CH_2Cl_2/MeOH) to give yellow crystals of $Ru_4(\mu_4\text{-}C_2)(\mu\text{-}PPh_2)_2(CO)_{12}$ (**11**) (12 mg, 18%). (Found: C, 40.15; H, 1.70. $C_{38}H_{20}O_{12}P_2Ru_4$ calc.: C, 40.22; H, 1.78%). IR (cyclohexane): ν(CO) 2091m, 2071s, 2057vs, 2020w, 2011m, 2000s, 1995w, 1985w cm^{-1}. ^1H NMR: δ ($CDCl_3$) 7.25 (m, Ph).

Conversion of 9 to 10. A solution of **9** (110 mg, 0.083 mmol) in benzene (50 ml) was carbonylated in an autoclave (12 atm, 70 °C, 22 h). Evaporation of the red solution and recrystallisation of the residue from CH_2Cl_2/MeOH under a CO atmosphere gave red crystals of **10** (60 mg, 55%), identified by comparison of its IR spectrum in the carbonyl region with that of the sample prepared above.

CO loss from 9. A solution of **9** (50 mg, 0.038 mmol) in CH_2Cl_2 (5 ml) was heated under reflux for 20 min. Addition of MeOH (5 ml) to the solution followed by concentration to ca. 5 ml and cooling to 0 °C gave black crystals of **2** (43 mg, 90%), identified by comparison of the carbonyl region of its IR spectrum with that for an authentic sample.

In solution **9** reverts to **2** within 2 h at room temperature.

CO loss from 10. A solution of **10** (50 mg, 0.038 mmol) in CH_2Cl_2 (10 ml) was heated at reflux point for 7 h, during which the solution gradually darkened from red to black. Addition of MeOH (10 ml), concentration to ca. 10 ml, and cooling to 0 °C gave black crystals of **2** (30 mg, 63%), identified as above.

Reactions of $Ru_5(\mu_5\text{-}\eta^2,P\text{-}C_2PPh_2)(\mu\text{-}PPh_2)(CO)_{13}$ with H_2

A. Under 10 atm. A solution of **2** (100 mg, 0.079 mmol) in cyclohexane (40 ml) was hydrogenated in an autoclave (10 atm, 25 °C, 18 h). The resulting burnt-yellow solution was evaporated to dryness and the residue subjected to preparative TLC (light petroleum/acetone 90/10) to give seven bands. Band 1, R_f 0.86, gave yellow $Ru_4(\mu\text{-}H)_2(CO)_{12}$ (9 mg, 16%) identified by comparison of the carbonyl region of its IR spectrum with that for an authentic sample. Band 3, R_f 0.48, yellow, recrystallised from CH_2Cl_2/MeOH to give yellow crystals of $Ru_4(\mu\text{-}H)_3(\mu_4\text{-}\eta^2,P\text{-}HC_2PPh_2)(\mu\text{-}PPh_2)(CO)_{10}$ (**12**) (52 mg, 63%), m.p. 161–164 °C. (Found: C, 39.98; H, 2.23; $C_{36}H_{24}O_{10}P_2Ru_4$ calc.: C, 39.93; H, 2.23%). IR(cyclohexane): ν(CO) 2097m, 2071s, 2038vs, 2024s, 2012m, 1987m, 1977m cm^{-1}. ^1H NMR: δ ($CDCl_3$) 7.24 (m, 20H, Ph), 9.10 [dd, J(PH) 2.6 and 18.1 Hz, 1H, C_2H], −15.40 (m, 1H, RuH), −18.53 [dm, J(PH) 24.0 Hz, 1H, RuH], −19.00 [dm J(PH) 18.9 Hz, 1 H, RuH). The remaining bands contained only trace amounts and were not identified.

B. At normal pressure. Hydrogen was passed through a solution of **2** (180 mg, 0.142 mmol) in refluxing cyclohexane (70 ml) for 5 h. Evaporation of the resulting red solution and preparative TLC (light petroleum/acetone 90/10) of the residue gave six bands. Band 1, R_f 0.81, yellow, $Ru_4(\mu\text{-}H)_4(CO)_{12}$ (trace). Band 2, R_f 0.50, pink (trace), not identified. Band 3, R_f 0.45, yellow, recrystallised from CH_2Cl_2/MeOH to give yellow crystals of $Ru_4(\mu\text{-}H)_3(\mu_4\text{-}\eta^2,P\text{-}HC_2PPh_2)(\mu\text{-}PPh_2)(CO)_{10}$ (**12**) (2 mg, 1%). Band 4, R_f 0.40, brown $Ru_5(\mu\text{-}H)(\mu_5\text{-}\eta^2,P\text{-}C{=}CHPPh_2)(\mu\text{-}PPh_2)(CO)_{13}$ (**13**) (trace). Band 5, R_f 0.30, orange, recrystallised from CH_2Cl_2/MeOH to give red crystals of $Ru_5C(\mu\text{-}H)_3(\mu\text{-}PPh_2)(CO)_{11}(PMePh_2)$ (**15**) (93 mg, 54%), m.p. 155–157 °C. (Found: C, 36.48; H, 1.86; $C_{37}H_{26}O_{11}P_2Ru_5$ calc.: C, 36.61; H, 2.16%). IR (cyclohexane): ν(CO) 2085s, 2055vs, 2032vs, 2020vs, 2002m, 1994w, 1989w, 1979m, 1945w cm^{-1}. ^1H NMR: δ ($CDCl_3$) 1.88 [d, J(PH) 7.7 Hz, 3H, CH_3], 7.27 (m, 20H, Ph), −19.97 (m, 2H, RuH), −22.50 (dm, J(PH) 17.9 Hz, 1H, RuH). Band 6, R_f 0.22, orange, recrystallised from CH_2Cl_2/MeOH to give dark red crystals of $Ru_5(\mu\text{-}H)_2(\mu_4\text{-}CCH_2PPh_2)(\mu\text{-}PPh_2)(CO)_{12}$ (**14**) (41 mg, 23%), m.p. 165–169 °C. (Found: C, 36.57, H, 1.59. $C_{38}H_{24}O_{12}P_2Ru_5$ calc.: C, 36.81; H, 1.95%). IR (cyclohexane): ν(CO) 2082m, 2058w, 2041m, 2028s, 2014(sh), 2004w, 1984m, 1977m cm^{-1}. ^1H NMR: δ ($CDCl_3$) 5.04 (m, ABX pattern, $J(H_AP)$ 10.3; $J(H_BP)$ 12.0, J(AB) 15.0 Hz, 2H, CH_2), 7.39 (m, 20H, Ph), −20.19 [dd, J(PH) 6.9 and 1.20 Hz, 2H, RuH]. Bands 1, 3 and 4 were identified by comparison of the carbonyl region of their IR spectra with those for authentic samples.

Shorter reaction times gave higher yields of **13** and **14** at the expense of **15**.

Hydrogenation of $Ru_5(\mu\text{-}H)(\mu_5\text{-}\eta^2,P\text{-}CCHPPh_2)(\mu\text{-}PPh_2)(CO)_{13}$ (13)

In a similar reaction, hydrogenation of **13** in refluxing cyclohexane (45 min) afforded, after preparative TLC, $Ru_5(\mu\text{-}H)_2(\mu_4\text{-}CCH_2PPh_2)(\mu\text{-}PPh_2)(CO)_{12}$ (**14**) (53%) and $Ru_5C(\mu\text{-}H)_3(\mu\text{-}PPh_2)(CO)_{11}(PMePh_2)$ (**15**) (21%), identified by comparison of their ν(CO) bands with those listed above.

Hydrogenation of $Ru_5(\mu\text{-}H)_2(\mu_4\text{-}CCH_2Pph_2)(\mu\text{-}PPh_2)(CO)_{12}$ (14)

In a similar reaction, hydrogenation of **14** in refluxing cyclohexane (2.5 h) afforded after crystallisation $Ru_5C(\mu\text{-}H)_3(\mu\text{-}PPh_2)(CO)_{11}(PMePh_2)$ (**15**) in 53% yield, identified as above.

Reaction of $Ru_5(\mu_5\text{-}\eta^2,P\text{-}C_2PPh_2)(\mu\text{-}PPh_2)(CO)_{13}$ (2) with $K[BHBu^s_3]$

A solution of **2** (50 mg, 0.04 mmol) in THF (5 ml) was treated with $K[BHBu^s_3]$ (0.10 ml of a 0.5 mol l^{-1} solution in THF, 0.05 mmol). After 5 min stirring at 25 °C, H_3PO_4 (2 drops) was added, and the solution was stirred for a further 5 min. The solvent was evaporated and the residue extracted with light petroleum (3 × 10 ml). The combined extracts were filtered and evaporated, and the residue was recrystallised from CH_2Cl_2/MeOH to give black crystals of $Ru_5(\mu\text{-}H)(\mu_5,\eta^2,P\text{-}C{=}CHPPh_2)(\mu\text{-}PPh_2)(CO)_{13}$ (**13**) (12 mg, 24%), m.p. > 200 °C. (Found: C, 36.71; H, 1.43; $C_{39}H_{22}O_{13}P_2Ru_5$ calc.: C, 37.00; H, 1.75%). IR (cyclohexane): ν(CO) 2084m, 2064s, 2029s, 2016s, 2002m, 1992vw, 1979w, 1965w, 1952w cm^{-1}. ^1H NMR: δ ($CDCl_3$) 5.86 [d, J(PH) 6.0 Hz, 1H, CH], 7.42 (m, 20H, Ph), −13.11 [dd, J(PH) 13.8 and 21.5 Hz, 1H, RuH].

Structure determinations

Unique data sets were measured at ~ 295 K within the specified $2\theta_{max}$ limit using Syntex $P\bar{1}$ and $P2_1$ four-circle diffractometers fitted with monochromatic Mo-K_α radiation sources (λ 0.7106_9 Å) and operating in conventional $2\theta/\theta$ scan mode. N independent reflections were obtained, N_o with $I > 3\sigma(I)$ being considered as observed and used in the full matrix least squares refinement after analytical absorption correction and solution of the structure by direct methods. Anisotropic thermal parameters were refined for the non-hydrogen atoms; $(x, y, x, U_{iso})_H$ were refined for the hydrogen atoms, except in the case of **14**, for which the crystal was of inferior quality, being split. In this case, H atom parameters for the organic components only were included at estimated values. Residuals at convergence are conventional R, R' on $|F|$; statistical weights were used, derived from $\sigma^2(I) = \sigma^2(I)_{diff} = 0.000n\sigma^4(I)_{diff}$. Neutral atom complex scattering factors were used [43]; computation used the XTAL program system implemented by S.R. Hall on a Perkin–Elmer 3240 computer. *N.B.* The atom numbering of **13** and **15** has been changed from that used originally [12] so that core identities are preserved through the reaction pathway (Scheme 2).

Crystal data

13: $Ru_5(\mu\text{-}H)(\mu_5\text{-}CCHPPh_2)(\mu\text{-}PPh_2)(CO)_{13} \equiv C_{39}H_{22}O_{13}P_2Ru_5$, $M = 1265.9$, Monoclinic, space group $P2_1/n$ (C^5_{2h}, No. 14(variant)), a 25.115(6), b 10.126(2), c 17.373(4) Å, β 109.88(2)°, U 4155(2) Å^3. D_c ($Z = 4$) = 2.02 g cm^{-3}. $F(000) = 2456$. μ_{Mo} 17.6 cm^{-1}. Specimen: 0.29 × 0.21 × 0.40 mm. $A^*_{min,max} = 1.37, 1.71$. $2\theta_{max}$ 65°, $N = 15106$, $N_0 = 9411$. $R = 0.038$, $R' = 0.032$, $n = 0.5$.

14: $Ru_5(\mu\text{-}H)_2(\mu_4\text{-}CCH_2PPh_2)(\mu\text{-}PPh_2)(CO)_{12} \equiv C_{38}H_{24}O_{12}P_2Ru_5$, $M =$ 1241.9, Triclinic, space group $P\bar{1}$ (C^1_i, No. 2), a 16.98(1), b 12.171(4), c 10.762(5) Å, α 71.16(4), β 87.20(4), γ 72.23(5)°, U 2002(1) Å^3, D_c ($Z = 2$) 2.06 g cm^{-1}. $F(000) = 1196$. μ_{Mo} 18.4 cm^{-1}. Specimen: 0.25 × 0.07 × 0.32 mm. $A^*_{min,max} = 1.14$, 1.64. $2\theta_{max}$ 60°. $N = 11083$, $N_0 = 6312$. $R = 0.063$, $R' = 0.085$, $n = 1.4$.

15: $Ru_5C(\mu\text{-}H)_3(\mu\text{-}PPh_2)(CO)_{11}(PMePh_2) \equiv C_{37}H_{26}O_{11}P_2Ru_5$, $M = 1213.9$, Triclinic, space group $P\bar{1}$, a 18.658(4), b 12.483(3), c 9.678(2) Å, α 69.13(2), β 78.21(2),

γ 73.19(2)°, U 2004(1) Å^3. D_c ($Z = 2$) 2.01 g cm^{-3}. $F(000) = 1172$. μ_{Mo} 18.2 cm^{-1}. Specimen: $0.06 \times 0.30 \times 0.30$ mm. $A^*_{min,max} = 1.11, 1.61$. $2\theta_{max}$ 65°. $N = 13079$, $N_0 = 10214$. $R = 0.026$, $R' = 0.029$, $n = 0.6$.

Acknowledgements

We thank the Australian Research Grants Scheme for support of this work. MLW held a Commonwealth Post-graduate Research Award.

References

1 M.I. Bruce, M.L. Williams, J.M. Patrick and A.H. White, J. Chem. Soc., Dalton Trans., (1985) 1229.
2 J.-C. Daran, O. Kristiansson and Y. Jeannin, C.R. Acad. Sci. Paris, 300 (1985) 943.
3 J.-C. Daran, Y. Jeannin and O. Kristiansson, Organometallics, 4 (1985) 1882.
4 J.-C. Daran, E. Cabrera, M.I. Bruce and M.L. Williams, J. Organomet. Chem., 319 (1987) 239.
5 A.J. Carty, S.A. MacLaughlin and N.J. Taylor, J. Am. Chem. Soc., 103 (1981) 2456.
6 S.A. MacLaughlin, N.J. Taylor and A.J. Carty, Organometallics, 3 (1984) 392.
7 A.J. Carty, Pure Appl. Chem., 54 (1982) 113.
8 J.S. Bradley, Adv. Organomet. Chem., 22 (1983) 1.
9 M.I. Bruce and M.L. Williams, J. Organomet. Chem., 282 (1985) C11.
10 M.I. Bruce, M.R. Snow, E.R.T. Tiekink and M.L. Williams, J. Chem. Soc., Chem. Commun., (1986) 701.
11 M.I. Bruce, M.L. Williams, B.W. Skelton and A.H. White, J. Organomet. Chem., 282 (1985) C53.
12 M.I. Bruce, B.W. Skelton, A.H. White and M.L. Williams, J. Chem. Soc., Chem. Commun., (1985) 744.
13 C. Barner-Thorsen, K.I. Hardcastle, E. Rosenberg, J. Siegel, A.M.M. Landford, A. Tiripicchio and M. Tiripicchio-Camellini, Inorg. Chem., 20 (1981) 4306.
14 F.W.B. Einstein, R.K. Pomeroy, P. Rushman and A.C. Willis, J. Chem. Soc., Chem.Commun., (1983) 854.
15 A.D. Harley, G.J. Guskey and G.L. Geoffroy, Organometallics, 2 (1983) 53; and ref. cited therein.
16 S.A. MacLaughlin, A.J. Carty and N.J. Taylor, Can. J. Chem., 60 (1982) 87.
17 A.J. Carty, S.A. MacLaughlin and N.J. Taylor, J. Organomet. Chem., 204 (1981) C27.
18 F. Baert, A. Guelzim and P. Coppens, Acta Crystallogr., B, 40 (1984) 590.
19 M. Catti, G.Gervasio and S.A. Mason, J. Chem. Soc., Dalton Trans., (1977) 2260.
20 J.M. Wisner, T.J. Bartczak and J.A. Ibers, Inorg. Chim. Acta, 100 (1985) 115; M.I. Bruce, M.G. Humphrey, M.R. Snow and E.R.T. Tiekink, J. Organomet. Chem., 314 (1986) 213.
21 M.L. Listermann and R.R. Schrock, Organometallics, 4 (1985) 75.
22 R. Toreki, R.E. LaPointe and P.T. Wolczanski, J. Am. Chem. Soc., 109 (1987) 7558.
23 M. Appel, J. Heidrich and W. Beck, Chem. Ber., 120 (1987) 1087.
24 H. Ogawa, T. Joh, S. Takahashi and K. Sonogashira, J. Chem. Soc., Chem. Commun., (1985) 1220.
25 R.J. Cross and M.F. Davidson, J. Chem. Soc., Dalton Trans., (1986) 411; M.I. Bruce, K.R. Grundy, M.J. Liddell, M.R. Snow and E.R.T. Tiekink, J. Organomet. Chem., 344 (1988) C49.
26 R.J. Blau, M.H. Chisholm, K. Folting and R.J. Wang, J. Am. Chem. Soc., 109 (1987) 4552.
27 M.I. Bruce, E. Horn, O. bin Shawkataly and M.R. Snow, J. Organomet. Chem., 280 (1985) 289.
28 B.F.G. Johnson, J. Lewis, J.N. Nicholls, J. Puga, P.R. Raithby, M.J. Rosales, M. McPartlin and W. Clegg, J. Chem. Soc., Dalton Trans., (1983) 277.
29 R. Markby, I. Wender, R.A. Friedel, F.A. Cotton and H.W. Sternberg, J. Am. Chem. Soc., 80 (1958) 6529; for reviews, see D. Seyferth, Adv. Organomet. Chem., 14 (1976) 97; R.D.W. Kemmitt and D.R. Russell, in G. Wilkinson, F.G.A. Stone and E.W. Abel (Eds.), Comprehensive Organometallic Chemistry, Pergamon, Oxford, 1982, Vol. 5, Chap. 34, p. 162.
30 F.G.A. Stone, Am. Chem. Soc. Symp. Ser., 211 (1983) 383.
31 D.L. Davies, J.C. Jeffery, D. Miguel, P. Sherwood and F.G.A. Stone, J. Chem. Soc., Chem. Commun., (1987) 454.
32 M.A. Beno, J.M. Williams, M. Tachikawa and E.L. Muetterties, J. Am. Chem. Soc., 103 (1981) 1485.
33 E. Roland, W. Bernhardt and H. Vahrenkamp, Chem. Ber., 118 (1985) 2858.

34 A.M. Bradford, M.C. Jennings and R.J. Puddephatt, Organometallics, 7 (1988) 792.
35 M. Castiglioni, G. Gervasio and E. Sappa, Inorg. Chim. Acta, 49 (1981) 217.
36 K. Kwek, N.J. Taylor and A.J. Carty, J. Am. Chem. Soc., 106 (1984) 4636.
37 B.F.G. Johnson, R.D. Johnston and J. Lewis, Chem. Commun., (1967) 1057; C.R. Eady, B.F.G. Johnson and J. Lewis, J. Chem. Soc., Dalton Trans., (1975) 2606.
38 M.I. Bruce, J.G. Matisons, J.R. Rodgers and R.C. Wallis, J. Chem. Soc., Chem. Commun., (1981) 1070.
39 R.D. Adams, P. Mathur and B.E. Segmüller, Organometallics, 2 (1983) 1258.
40 Y. Degani and I. Willner, J. Chem. Soc., Chem. Commun., (1985) 648.
41 M.I. Bruce, J.G. Matisons, R.C. Wallis, J.M. Patrick, B.W. Skelton and A.H. White, J. Chem. Soc., Dalton Trans., (1983) 2365.
42 M.I. Bruce, J.G. Matisons and B.K. Nicholson, J. Organomet. Chem., 247 (1983) 321.
43 J.A. Ibers and W.C. Hamilton, International Tables for X-ray Crystallography, vol. 4, Kynoch Press, Birmingham, 1974.
44 M.I. Bruce, M.J. Liddell, O. bin Shawkataly, I.R. Bytheway, B.W. Skelton and A.H. White, J. Organomet. Chem., 369 (1989) 217.